IOP Publishing Journal of Physics A: Mathematical and Theoretical

J. Phys. A: Math. Theor. **53** (2020) 075201 (36pp) https://doi.org/10.1088/1751-8121/ab604c

Families of two-dimensional Coulomb gases on an ellipse: correlation functions and universality

Taro Nagao[1,4], **Gernot Akemann**[2], **Mario Kieburg**[2,3] and **Iván Parra**[2]

[1] Graduate School of Mathematics, Nagoya University, Chikusa-ku, Nagoya 464-8602, Japan
[2] Faculty of Physics, Bielefeld University, D-33501 Bielefeld, Germany
[3] School of Mathematics and Statistics, The University of Melbourne, Parkville, VIC 3010, Australia

E-mail: nagao@math.nagoya-u.ac.jp

Received 4 June 2019, revised 29 November 2019
Accepted for publication 10 December 2019
Published 22 January 2020

Abstract

We investigate a one-parameter family of Coulomb gases in two dimensions, which are confined to an ellipse due to a hard wall constraint, and are subject to an additional external potential. At inverse temperature $\beta = 2$ we can use the technique of planar orthogonal polynomials, borrowed from random matrix theory, to explicitly determine all k-point correlation functions for a fixed number of particles N. These are given by the determinant of the kernel of the corresponding orthogonal polynomials, which in our case are the Gegenbauer polynomials, or a subset of the asymmetric Jacobi polynomials, depending on the choice of external potential, as shown in a companion paper recently published by three of the authors. In the rotationally invariant case, when the ellipse becomes the unit disc, our findings agree with that of the ensemble of truncated unitary random matrices. The thermodynamical large-N limit is investigated in the local scaling regime in the bulk and at the edge of the spectrum at weak and strong non-Hermiticity. We find new universality classes in these limits and recover the sine- and Bessel-kernel in the Hermitian limit. The limiting global correlation functions of particles in the interior of the ellipse are more difficult to obtain but found in the special cases corresponding to the Chebyshev polynomials.

Keywords: two-dimensional Coulomb gas, planar orthogonal polynomials, weak non-Hermiticity, universality

(Some figures may appear in colour only in the online journal)

[4] Author to whom any correspondence should be addressed.

1. Introduction

Coulomb gases in two dimensions are constituted by a set of particles that interact logarithmically and that are subject to some confining potential, that may for example be given by a Gaussian or a hard wall constraint on a certain domain. At specific values of the temperature $T = 1/(k_B\beta)$ (with the Boltzmann constant k_B) they can be studied using non-Hermitian random matrix theory (RMT), where the complex matrix eigenvalues represent the locations of the charged particles. The three classical Ginibre ensembles [1] for instance, which all have a Gaussian potential, correspond to one-component plasmas with a suitable background charge, see [2, 3].

On the one hand, Coulomb gases at general temperature β are objects of intense study and pose challenging open problems, e.g. the formation of the so-called Abrikosov lattice at large β, and we refer to [4] for a review. Typically, for large systems of $N \gg 1$ particles with $\beta \sim \mathcal{O}(1)$, the eigenvalues condense into a droplet, the circular law for the rotationally invariant Gaussian potential, and local fluctuations around this density as well as higher order correlation functions are of interest. The case of a growing droplet where particles are constantly fed in has applications to viscous fluids, or more generally can be viewed as Laplacian growth models [5]. The case of a hard wall imposed at the edge of the droplet has been studied in [6]. When forcing the gas away from its equilibrium position, phase transitions may occur, see [7] for more general potentials and the general situation in d dimensions. Likewise, when $\beta = 2c/N \to 0$ at fixed c, a smooth transition to a Gaussian is observed [8], including the weakly attractive case $c \in (-2, 0]$.

On the other hand, the specific value of $\beta = 2$ that is tractable via RMT enjoys an exact analytical solution for finite N. Moreover, these examples find themselves in various applications e.g. in scattering in open quantum systems or in quantum field theories with chemical potential, see [9] and [10] for respective reviews. A powerful technique providing an exact solution of such Coulomb gases uses orthogonal polynomials in the complex plane. Exploiting the fact that at $\beta = 2$ the joint density of complex eigenvalues forms a determinantal point process, one can explicitly construct the kernel of such planar polynomials and thus determine all eigenvalue correlation functions. Taking the complex elliptic Ginibre ensemble as an example, which is not rotationally invariant and supported on the full complex plane $\mathbb{C}$, these planar polynomials are provided by the Hermite polynomials [11]. They are orthogonal with respect to a Gaussian weight function, with different variances in real and imaginary parts [12, 13]. Based on the explicit solution for the kernel various large-N limits can be taken. At strong non-Hermiticity, the global eigenvalue density condenses onto an ellipse in the complex plane. Nevertheless, the local eigenvalue correlation functions at the edge and in the bulk of the spectrum agree with that of the rotationally invariant complex Ginibre ensemble. In fact much further reaching universality results for complex Wigner ensembles are known [14].

A particularly interesting limit called weak non-Hermiticity was introduced in [15] for the elliptic Ginibre ensemble. Whereas in this limit the global density collapses to the semicircle on the real line, locally correlations of $\mathcal{O}(1/N)$ still extend into the complex plane. In the bulk the limiting kernel at weak non-Hermiticity is a one-parameter deformation of the celebrated sine-kernel, known from one-dimensional Wigner–Dyson statistics in RMT, which is highly universal [16]. The universality of this deformed, weakly non-Hermitian kernel was first shown heuristically in [11], using supersymmetry for independent matrix elements, and more recently proven for a class of non-Gaussian deformations [17], including fixed trace ensembles which are non-determinantal. This concept of weak non-Hermiticity was applied to other ensembles [18, 19] and different scaling limits were found also at hard [18, 19] and soft edges [20] of the spectrum, see [21] for a list of many known kernels that deform the three classical ensembles and their chiral counterparts. For the scaling limit in the vicinity of a cusp or close to a hard wall we refer to [6, 22].

In this paper we will take the large-N limit of a new class of Coulomb gases that are confined by a hard wall constraint to live on an ellipse at finite-N already, subject to an additional potential. The solution is based on another class of classical orthogonal polynomials that were shown in a companion paper [23] to be orthogonal on such a domain, subject to certain families of external potentials: the Gegenbauer (or ultraspherical) polynomials, which are the Jacobi polynomials with symmetric indices, and a subset of the Jacobi polynomials with unequal ones. At present we do not have a non-trivial random matrix representation for the determinantal point process solved by these polynomials. Only in the rotationally invariant case, when the ellipse degenerates to the unit disc, it follows from the complex eigenvalue distribution of truncated unitary matrices, with monomial orthogonal polynomials [18].

The outline of this paper is the following. In section 2 we introduce the family of Coulomb gases that we will study and discuss limiting cases to known results in two and one dimensions. Section 3 reviews the determinantal structure of these at the special inverse temperature $\beta = 2$, see [23]. The corresponding planar orthogonal Gegenbauer polynomials and their corresponding kernel are presented. The limits to known kernels are given, in order to prepare a later comparison of the microscopic kernels. Section 4 comes to our new results and is devoted to the local, microscopic correlations in the weak non-Hermiticity limit. Section 4.1 deals with the scaling limit in the bulk, close to the origin, then turning to the edge scaling limit in section 4.2. In both limits we find new one-parameter universality classes deforming the sine- and Bessel-kernel that we recover in the Hermitian limit. A large weak non-Hermiticity parameter is known to lead to strong non-Hermiticity, which we thus explore indirectly. In the bulk we find a new limiting kernel as well, and recover a well-known bulk result (the Ginibre kernel) in a limit of a potential parameter. At the edge, on the other hand, we recover the result from the truncated unitary matrix ensemble. As a further check the edge kernel is found to be asymptotically similar to the bulk kernel, thus underlining its conjectured universality. The global large-N limit is addressed in section 5 for a special case of the Chebyshev polynomials of the second kind, being orthogonal with respect to the flat measure [29]. Two families of the non-symmetric Jacobi polynomials and their corresponding Coulomb gases that were introduced in [23] for finite N are analysed in appendix A, giving rise to two further local universality classes at the edge. In appendices B and C, the global regime is again considered for Coulomb gases related to the remaining Chebyshev polynomials that were known to be orthogonal, see [30].

2. A family of Coulomb gases on an ellipse

In this section we will introduce the particular Coulomb gas that we will investigate. We also point out limits to systems of charged particles previously known from RMT. Let us consider a two-dimensional, static one-component Coulomb gas with a Hamiltonian

$$H = \sum_{j=1}^{N} V(z_j) - \sum_{j<l}^{N} \log|z_j - z_l| \,. \tag{2.1}$$

The locations of the particles interacting logarithmically in the plane are denoted by complex numbers $z_j = x_j + \mathrm{i}y_j$ $(j = 1, 2, \cdots, N)$ with the standard map $(x_j, y_j) \in \mathbb{R}^2 \mapsto z_j \in \mathbb{C}$. We impose the particles to be confined to an ellipse, which is given in the following parametrisation.

$$E = \left\{ z = x + \mathrm{i}y \,\middle|\, \frac{2\tau}{1+\tau}x^2 + \frac{2\tau}{1-\tau}y^2 \leqslant 1 \right\}, \quad 0 < \tau < 1. \tag{2.2}$$

Here x and y are real. The one-particle potential in the Hamiltonian (2.1) is given by

$$V(z) = -\frac{a}{2}\log\left(1 - \frac{2\tau}{1+\tau}x^2 - \frac{2\tau}{1-\tau}y^2\right), \quad a > -1\ . \tag{2.3}$$

This potential mimics a charged mirror at the boundary of the ellipse which is either attractive ($a < 0$) or repulsive ($a > 0$). The resulting probability distribution function for the particles to be at equilibrium at an inverse temperature $1/(k_\mathrm{B}T) = \beta = 2$ is known to be

$$P(z_1, z_2, \cdots, z_N) = \frac{1}{Z_N}\mathrm{e}^{-\beta H} = \frac{1}{Z_N}\prod_{j=1}^{N} w(z_j)\prod_{j<l}^{N}|z_j - z_l|^2\ . \tag{2.4}$$

Here, we define a one-particle weight function

$$w(z) = \left(1 - \frac{2\tau}{1+\tau}x^2 - \frac{2\tau}{1-\tau}y^2\right)^a = \mathrm{e}^{-\beta V(z)}, \tag{2.5}$$

which is real and non-negative, $w(z) = w(\bar{z}) \geqslant 0$ ($\forall z \in E$), and use the integration measure $\prod_{j=1}^{N}\mathrm{d}^2 z_j = \prod_{j=1}^{N}\mathrm{d}x_j\mathrm{d}y_j$. The notation $\bar{z}$ denotes the complex conjugate of z. The point process in (2.4) is determinantal, as shown in section 3, see [23]. The partition function that normalises the distribution (2.4) is defined as

$$Z_N = \prod_{j=1}^{N}\int_E \mathrm{d}^2 z_j\, w(z_j)\prod_{i<l}^{N}|z_i - z_l|^2\ . \tag{2.6}$$

Let us point out several limits of the distribution (2.4) known from RMT. First, we consider the rotationally invariant limit. Here, we have to rescale the positions as

$$x_j \mapsto x_j/\sqrt{2\tau}, \quad y_j \mapsto y_j/\sqrt{2\tau}, \tag{2.7}$$

and then take the limit $\tau \to 0$. In this limit the ellipse E in (2.2) becomes the unit disc. The limiting weight function becomes

$$w_{\mathrm{truncated}}(z) = \left(1 - |z|^2\right)^a, \quad a > -1, \tag{2.8}$$

which is radially symmetric. For an integer a the limiting joint density from (2.4) then agrees with the distribution of the complex eigenvalues of the ensemble of truncated unitary random matrices introduced in [18]. It is obtained from a unitary matrix $U \in U(N)$ distributed according to the Haar measure, truncated to the upper left block of U of size $M \times M$, with $N > M$ and the resulting parameter

$$a = N - M - 1\ . \tag{2.9}$$

The complex eigenvalue correlation functions of such a truncated unitary matrix were computed in [18], using monomials $M_n(z) = z^n$ as orthogonal polynomials with respect to the weight (2.8).

In the second limit, we want to make contact with the eigenvalues of Hermitian RMT and the corresponding Dyson gas of particles confined to (a subset of) the real line, while still interacting logarithmically, that is with Coulomb interaction in two dimensions. Taking the limit $\tau \to 1$ on the ellipse E in (2.2) enforces the imaginary part to condense on a narrow strip about the real line and eventually to vanish, $y \to 0$, and thus maps E to the interval $[-1, 1]$. Because the initial measure is in two dimensions, in (2.4) we still have to integrate out the imaginary parts $\Im(z_j) = y_j$, leading to an additional contribution to the weight function, see [23, remark 3.7] for details. We arrive at the following limiting weight function

$$w_{\text{Jacobi}}(x) = \left(1 - x^2\right)^{a+\frac{1}{2}}, \tag{2.10}$$

with joint density (2.4) projected to the real parts $\Re(z_j) = x_j \in [-1, 1]$ ($j = 1, 2, \cdots, N$). It agrees with a special case of the weight where the eigenvalues result from the Jacobi ensemble of Hermitian random matrices [24, 25]. The eigenvalue correlation functions are computed with the help of the Jacobi polynomials, in our case with symmetric indices, when the Jacobi polynomials reduce to the Gegenbauer polynomials (also called the ultraspherical polynomials). At $a = 0$ these become the Chebyshev polynomials of the second kind.

Finally, as also pointed out in [23], a map to the elliptic Ginibre ensemble exists, thus removing the hard wall constraint, with E becoming the entire complex plane after rescaling. This is achieved by making the scaling transformations (for $a > 0$)

$$x_j \mapsto x_j/\sqrt{2\tau a}, \quad y_j \mapsto y_j/\sqrt{2\tau a}, \tag{2.11}$$

and then taking the limit $a \to \infty$. Hence, the particles are pushed away from the boundary until it has no contact at all. Due to the scaling we zoom into the origin and find the limiting weight function (2.5) which is a Gaussian,

$$w_{\text{Ginibre}}(z) = \exp\left(-\frac{1}{1+\tau}x^2 - \frac{1}{1-\tau}y^2\right). \tag{2.12}$$

The resulting limiting distribution (2.4) agrees with that of the complex eigenvalues of the elliptic Ginibre ensemble of complex random matrices [26], including the rotationally invariant Ginibre ensemble at $\tau = 0$. The elliptic Ginibre ensemble was analysed as a Coulomb gas in [13], deriving and using the orthogonality property of the Hermite polynomials with respect to the weight (2.12). All complex eigenvalue correlation functions of the elliptic Ginibre ensemble were derived later in [11].

The rotationally invariant limit (2.8) and the real limit (2.10) will provide us with consistency checks for our Coulomb gas in the large-N limit, and lead to a better understanding of the issue of universality. A comparison to the elliptic Ginibre ensemble is more difficult which is related to the fact that its initial support is the full complex plane. Even after taking the large-N limit, the correlations at the edge of the limiting elliptic support only decay exponentially, in contrast to the hard constraint present in our case. This difference will be discussed in more detail in section 4.1.

3. Density correlation functions at finite-*N*

Let us recall that the probability distribution functions of the form (2.4) with $\beta = 2$ is a determinantal point process. Thus all density correlation functions are given in terms of a kernel of orthogonal polynomials in the complex plane. Suppose that the polynomials $M_n(z) = z^n + \mathcal{O}(z^{n-1})$ in monic normalisation satisfy the following orthogonality relation

$$\int_D \mathrm{d}^2 z\, w(z) M_m(z) M_n(\bar{z}) = h_n \delta_{m,n}, \quad m, n = 0, 1, 2, \cdots, \tag{3.1}$$

for a given non-negative weight function w on some domain D. Here, $z = x + \mathrm{i}y$ (x and y are real) and $\mathrm{d}^2 z = \mathrm{d}x\mathrm{d}y$. In our case the integration domain D is given by the ellipse E in (2.2), and the weight function $w(z)$ (satisfying $w(z) = w(\bar{z})$) is (2.5). Then, in general the k-point density correlation function defined as

$$\rho(z_1, z_2, \cdots, z_k) = \frac{N!}{(N-k)!} \int_D \mathrm{d}^2 z_{k+1} \int_D \mathrm{d}^2 z_{k+2} \cdots \int_D \mathrm{d}^2 z_N P(z_1, z_2, \cdots, z_N), \tag{3.2}$$

can be written in a determinantal form, in terms of the kernel K_N of these polynomials $M_n(z)$ from (3.1), see [27]:

$$\rho(z_1, z_2, \cdots, z_k) = \det\left[K_N(z_j, z_l)\right]_{j,l=1,2,\cdots,k}. \tag{3.3}$$

Here, the kernel is given by the sum over the orthonormalised polynomials,

$$K_N(z_j, z_l) = \sqrt{w(z_j)w(\bar{z}_l)} \sum_{n=0}^{N-1} \frac{1}{h_n} M_n(z_j) M_n(\bar{z}_l). \tag{3.4}$$

Therefore, in order to see the asymptotic behaviour of the correlation functions in any particular limit $N \to \infty$, we only need to evaluate the limit of the kernel $K_N(z_1, z_2)$.

Let us now specify the polynomials for our elliptic domain (2.2). In [23] the following orthogonality relation was proven[5]:

$$\begin{aligned}\int_E \mathrm{d}^2 z \left(1 - \frac{2\tau}{1+\tau}x^2 - \frac{2\tau}{1-\tau}y^2\right)^a C_m^{(a+1)}(z) C_n^{(a+1)}(\bar{z}) \\ = \frac{\sqrt{1-\tau^2}}{2\tau} \frac{\pi}{n+a+1} C_n^{(a+1)}\left(\frac{1}{\tau}\right) \delta_{m,n}, \quad a > -1,\end{aligned} \tag{3.5}$$

for $m, n = 0, 1, 2, \cdots$ on the ellipse E in (2.2). The polynomials $C_n^{(a+1)}$ are the Gegenbauer polynomials given by

$$C_n^{(a+1)}(z) = \sum_{j=0}^{\lfloor n/2 \rfloor} \frac{(-1)^j \Gamma(n+a-j+1)}{\Gamma(a+1)\Gamma(j+1)\Gamma(n-2j+1)} (2z)^{n-2j}, \tag{3.6}$$

where $\lfloor n/2 \rfloor$ is the floor function, meaning the greatest integer that is less than or equal to $n/2$. Equivalently, they can be expressed in terms of Gauß' hypergeometric function, or in terms of the Jacobi polynomials [28]

$$P_n^{(\alpha,\gamma)}(z) = \frac{1}{(1-z)^\alpha (1+z)^\gamma} \frac{(-1)^n}{2^n n!} \frac{d^n}{\mathrm{d}z^n} \left[(1-z)^{n+\alpha}(1+z)^{n+\gamma}\right], \tag{3.7}$$

with symmetric indices $\alpha = \gamma = a + \frac{1}{2}$, see (3.17) below. In particular they have parity symmetry, $C_n^{(a+1)}(-z) = (-1)^n C_n^{(a+1)}(z)$. We find that the corresponding monic orthogonal polynomials read

$$M_n(z) = \frac{\Gamma(a+1)\Gamma(n+1)}{\Gamma(n+a+1)2^n} C_n^{(a+1)}(z), \tag{3.8}$$

and that the normalisation constants resulting from (3.5) are obtained as

$$h_n = \frac{\Gamma(a+1)\Gamma(n+1)}{\Gamma(n+a+2)2^n} \frac{\pi\sqrt{1-\tau^2}}{2\tau} M_n\left(\frac{1}{\tau}\right). \tag{3.9}$$

Notice that for $n = 0$ we obtain the normalisation of our weight over E,

$$A = \int_E \mathrm{d}^2 z \left(1 - \frac{2\tau}{1+\tau}x^2 - \frac{2\tau}{1-\tau}y^2\right)^a = \frac{1}{a+1} \frac{\pi\sqrt{1-\tau^2}}{2\tau}. \tag{3.10}$$

[5] Compared to [23] where the ellipse is parametrised by $(x/a)^2 + (y/b)^2 \leqslant 1$ with $a > b > 0$, we have chosen a one-parameter family, setting $a^2 = (1+\tau)/2\tau$ and $b^2 = (1-\tau)/2\tau$ and thus $a^2 - b^2 = 1$, with foci located at $z = \pm 1$.

In [23] the orthogonality of two families of the Jacobi polynomials with non-symmetric indices on an ellipse was also derived. Their analysis is deferred to appendix A.

In the special case $a = 0$, when the Gegenbauer polynomials reduce to the Chebyshev polynomials of the second kind, $U_n(z) = C_n^{(1)}(z)$, the proof of the orthogonality relation (3.5) was previously known, see [29, 30]. It follows that the kernel $K_N(z_1, z_2)$ of the orthonormalised Gegenbauer polynomials is given by

$$K_N(z_1, z_2) = \left(1 - \frac{2\tau}{1+\tau}x_1^2 - \frac{2\tau}{1-\tau}y_1^2\right)^{a/2} \left(1 - \frac{2\tau}{1+\tau}x_2^2 - \frac{2\tau}{1-\tau}y_2^2\right)^{a/2} \times \frac{2\tau}{\pi\sqrt{1-\tau^2}} \sum_{n=0}^{N-1} \frac{n+a+1}{C_n^{(a+1)}(1/\tau)} C_n^{(a+1)}(z_1) C_n^{(a+1)}(\bar{z}_2) \,. \tag{3.11}$$

This completes the computation of all correlation functions via (3.3) for finite-N.

Before evaluating the asymptotic of this kernel in various limits $N \to \infty$ in the following sections, let us show how the kernel reduces to known limiting cases at finite-N, the rotationally invariant case and the Hermitian limit.

We begin with the rotationally invariant limit. After the rescaling (2.7) and sending $\tau \to 0$, we map the ellipse (2.2) to the unit disc, $E \to \{z = x + \mathrm{i}y \,|\, x^2 + y^2 \leqslant 1\}$. The orthogonal polynomials of the limiting weight function (2.8) are now monomials, $M_n(z) = z^n$, and the orthogonality relation is given by

$$\int_{|z|\leqslant 1} \mathrm{d}^2 z (1 - |z|^2)^a z^m \bar{z}^n = h_n^{\text{truncated}} \delta_{m,n}, \tag{3.12}$$

with norms

$$h_n^{\text{truncated}} = \pi \frac{\Gamma(a+1)\Gamma(n+1)}{\Gamma(n+a+2)} \,. \tag{3.13}$$

For the limit of the kernel (3.11) we obtain

$$\begin{aligned} K_N^{\text{truncated}}(z_1, z_2) &= \lim_{\tau \to 0} \frac{1}{2\tau} K_N\left(\frac{z_1}{\sqrt{2\tau}}, \frac{z_2}{\sqrt{2\tau}}\right) \\ &= (1 - |z_1|^2)^{\frac{a}{2}} (1 - |z_2|^2)^{\frac{a}{2}} \sum_{n=0}^{N-1} \frac{\Gamma(n+a+2)}{\pi\Gamma(a+1)\Gamma(n+1)} (z_1 \bar{z}_2)^n. \end{aligned} \tag{3.14}$$

For non-negative integer values of a it agrees with the kernel derived in [18] for the ensemble of truncated unitary random matrices, with relation (2.9) between the parameter a and the matrix dimensions. The rescaled 1-point density correlation functions (particle densities) describing the approach to the rotationally invariant limit $\tau \to 0$ are illustrated in figure 1. As the plot clearly highlights the spectrum concentrates on the one-dimensional ellipse and has only exponential tails into its interior.

In the Hermitian limit $\tau \to 1$ the ellipse (2.2) is mapped to $[-1, 1]$. In order to be able to take the limit of the orthogonality relation (3.1), with (3.8) and (3.9), we have to divide the orthogonality relation by the normalisation A from (3.10), yielding the normalised integral, see [23]

$$1 = \lim_{\tau \to 1} \frac{1}{A} \int_E \mathrm{d}^2 z \left(1 - \frac{2\tau}{1+\tau}x^2 - \frac{2\tau}{1-\tau}y^2\right)^a = \frac{1}{B} \int_{-1}^{1} \mathrm{d}x (1 - x^2)^{a+\frac{1}{2}}, \tag{3.15}$$

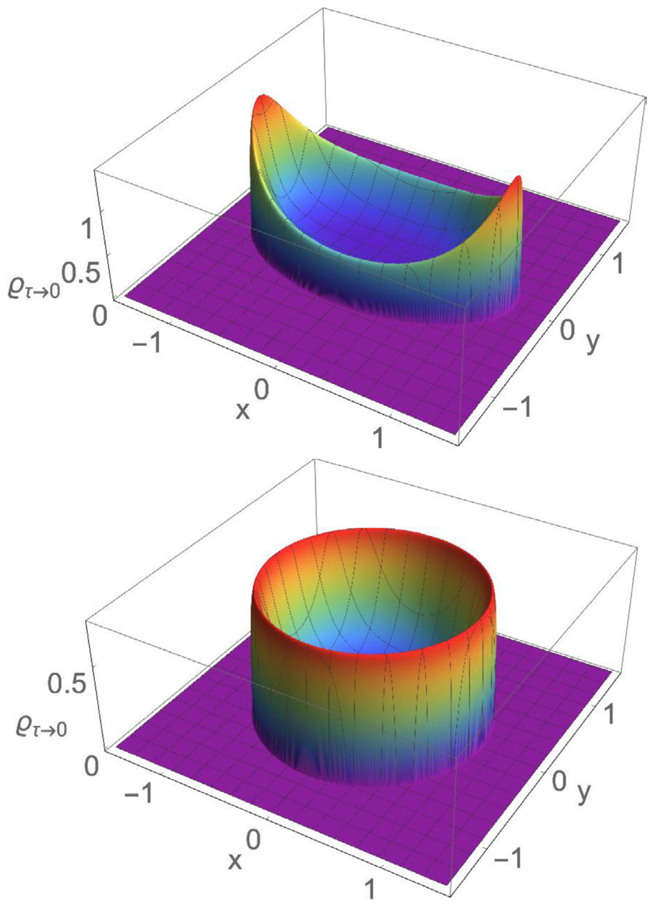

Figure 1. The rescaled particle densities $\rho_{\tau\to 0} = \frac{1}{2\tau N}\ K_N\left(\frac{x+\mathrm{i}y}{\sqrt{2\tau}}, \frac{x+\mathrm{i}y}{\sqrt{2\tau}}\right)$ for $N = 10$, $a = 1$, and $\tau = 0.5$ (upper figure) as well as $\tau = 0.005$ (lower figure).

with

$$B = \frac{\sqrt{\pi}\Gamma\left(a+\frac{3}{2}\right)}{\Gamma(a+2)}\ . \tag{3.16}$$

The limit $\tau \to 1$ of the monic polynomials $M_n(z)$ is non-singular (and remains monic), and due to the relation between the Gegenbauer and Jacobi polynomials with symmetric indices [31],

$$C_n^{(a+1)}(z) = \frac{\Gamma(n+2a+2)\Gamma\left(a+\dfrac{3}{2}\right)}{\Gamma(2a+2)\Gamma\left(n+a+\dfrac{3}{2}\right)} P_n^{(a+\frac{1}{2},\, a+\frac{1}{2})}(z), \tag{3.17}$$

they can also be expressed in terms of the latter,

$$M_n(z) = \frac{2^n\Gamma(n+1)\Gamma(n+2a+2)}{\Gamma(2n+2a+2)} P_n^{(a+\frac{1}{2},\, a+\frac{1}{2})}(z)\ . \tag{3.18}$$

It remains to evaluate $M_n(1)$ in the limiting norms (3.9), where we can use [31]

$$C_n^{(a+1)}(1) = \frac{\Gamma(n+2a+2)}{\Gamma(2a+2)\Gamma(n+1)}, \tag{3.19}$$

together with (3.8). Inserting all ingredients, using the doubling formula for the Gamma function

$$\sqrt{\pi}\Gamma(2z) = 2^{2z-1}\Gamma(z)\Gamma\left(z+\frac{1}{2}\right), \tag{3.20}$$

and multiplying with B after taking the limit (3.15), we arrive at the following orthogonality relation for the weight (2.10)

$$\int_{-1}^{1} \mathrm{d}x(1-x^2)^{a+\frac{1}{2}} M_m(x)M_n(x) = h_n^{\mathrm{Jacobi}}\delta_{m,n}, \tag{3.21}$$

with

$$h_n^{\mathrm{Jacobi}} = \frac{\pi\Gamma(n+1)\Gamma(n+2a+2)}{2^{2n+2a+1}\Gamma(n+a+2)\Gamma(n+a+1)} . \tag{3.22}$$

Together with (3.18) this agrees with the standard orthogonality relation of the Jacobi polynomials [3]. We have drawn the rescaled 1-point density correlation functions (particle densities) for this limit in figure 2. The spectrum evidently concentrates on the two extremal points $z = \pm 1$ because the Hermitian Jacobi ensemble, to which it converges, has square root singularities at these points.

It is also possible to recover the Hermite polynomials $H_n(z)$, which are orthogonal with respect to the weight (2.12) in the full complex plane [13], after taking the scaling limit $a \to \infty$ with (2.11). This limit to the elliptic Ginibre ensemble requires more preparation. While the limit of Gegenbauer polynomials with rescaled argument, as required by (2.11), is well-known [31, 18.7.24]:

$$\lim_{a\to\infty} a^{-n/2} C_n^{(a)}(z/\sqrt{a}) = \frac{1}{n!}H_n(z), \tag{3.23}$$

for the norm (3.9) we also need the corresponding limit *without* rescaling the arguments. It follows from the generating function for Gegenbauer polynomials [31, 18.12.4]

$$\sum_{n=0}^{\infty} C_n^{(a)}(x)r^n = (1-2rx+r^2)^{-a} . \tag{3.24}$$

After rescaling $r \to r/a$ and taking $a \to \infty$,

$$\lim_{a\to\infty} \sum_{n=0}^{\infty} \frac{1}{a^n} C_n^{(a)}(x)r^n = \mathrm{e}^{2rx} = \sum_{n=0}^{\infty} \frac{(2x)^n}{n!} r^n, \tag{3.25}$$

we obtain the relation

$$\lim_{a\to\infty} a^{-n} C_n^{(a)}(x) = \frac{1}{n!}(2x)^n . \tag{3.26}$$

Note the difference in the power of a compared to (3.23). Putting these together and rescaling as in (2.11), we obtain

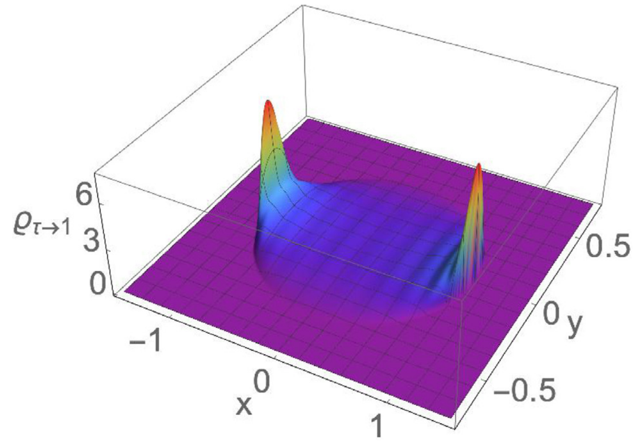

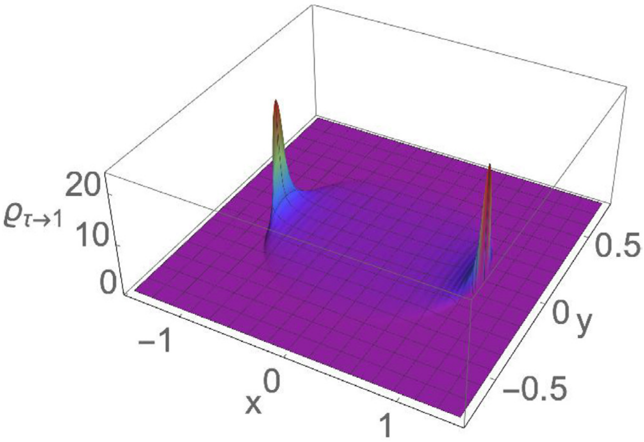

Figure 2. The rescaled particle densities $\rho_{\tau\to1} = \frac{1}{N^2} K_N\left(x + \mathrm{i}\frac{y}{N}, x + \mathrm{i}\frac{y}{N}\right)$ for $a = 1$, $\tau = \left(1 + \frac{s^2}{2N^2}\right)^{-1}$ with $s = 1$, and $N = 10$ (upper figure) as well as $N = 30$ (lower figure).

$$K_N^{\mathrm{Ginibre}}(z_1, z_2) = \lim_{a\to\infty} \frac{1}{2\tau a} K_N\left(\frac{z_1}{\sqrt{2\tau a}}, \frac{z_2}{\sqrt{2\tau a}}\right)$$
$$= \exp\left[-\frac{x_1^2}{2(1+\tau)} - \frac{y_1^2}{2(1-\tau)} - \frac{x_2^2}{2(1+\tau)} - \frac{y_2^2}{2(1-\tau)}\right]$$
$$\times \frac{1}{\pi\sqrt{1-\tau^2}} \sum_{n=0}^{N-1} \left(\frac{\tau}{2}\right)^n \frac{1}{n!} H_n\left(\frac{z_1}{\sqrt{2\tau}}\right) H_n\left(\frac{\bar{z}_2}{\sqrt{2\tau}}\right). \quad (3.27)$$

It agrees with the kernel of the elliptic Ginibre ensemble [11]. The Hermite polynomials satisfy [12, 13]

$$\int_{\mathbb{C}} \mathrm{d}^2 z \exp\left[-\frac{x^2}{1+\tau} - \frac{y^2}{1-\tau}\right] H_n\left(\frac{z}{\sqrt{2\tau}}\right) H_m\left(\frac{\bar{z}}{\sqrt{2\tau}}\right) = h_n^{\mathrm{Ginibre}} \delta_{n,m},$$
$$h_n^{\mathrm{Ginibre}} = n! \pi \sqrt{1-\tau^2} \left(\frac{\tau}{2}\right)^{-n}, \quad (3.28)$$

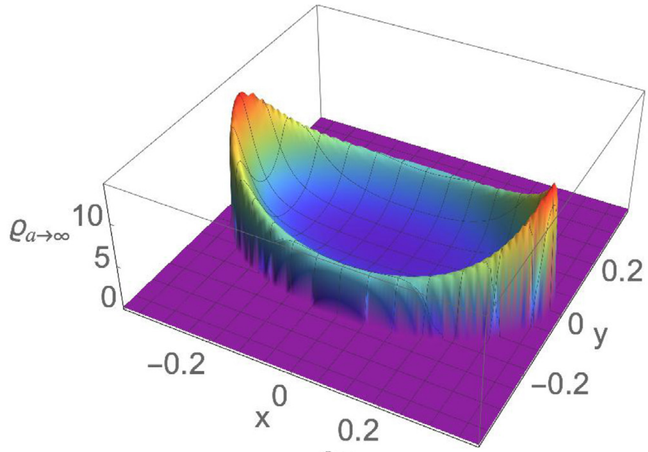

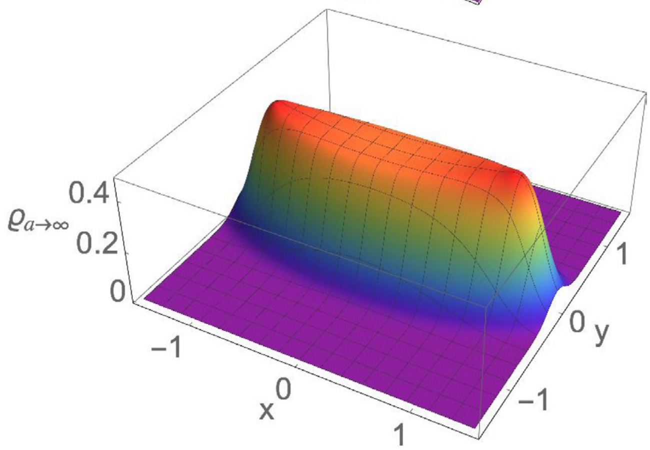

Figure 3. The rescaled particle densities $\rho_{a\to\infty} = \frac{1}{2\tau a} K_N\left(\frac{\sqrt{N}(x+\mathrm{i}y)}{\sqrt{2\tau a}}, \frac{\sqrt{N}(x+\mathrm{i}y)}{\sqrt{2\tau a}}\right)$ for $N = 10$, $\tau = 0.5$, and $a = 1$ (upper figure) as well as $a = 100$ (lower figure).

for $0 < \tau < 1$. As before, we illustrated the rescaled 1-point density correlation functions (particle densities) in the limit to the elliptic Ginibre ensemble $a \to \infty$, see figure 3. This time the spectrum fills out the whole ellipse so that a well defined bulk is available.

4. Local correlations at weak non-Hermiticity

In this section we come to our new results and will mainly be concerned with local correlation functions in the weakly non-Hermitian situation. For a discussion of strong non-Hermiticity we refer to the respective sections 4.1 and 4.2. With weak non-Hermiticity we mean a double scaling limit $N \to \infty$ and $\tau \to 1$, the Hermitian limit, taken such that the global density collapses to the real line, the interval $[-1, 1]$ in our case, whereas local correlation functions still extend into the complex plane. In the elliptic Ginibre ensemble the phenomenon of weak non-Hermiticity happens at different scales in N in the bulk [11] and at the soft edge [20] of the spectrum. In contrast, in our Coulomb gas living on a finite ellipse this happens on the *same* scale in N, that is $\tau = 1 - O(1/N^2)$. In our ensemble, with edge we mean the vicinity of the endpoints ± 1, and with bulk we mean the vicinity of interior points of the open interval

$(-1, 1)$, away from the edges. In view of the fact that for $a = O(1)$ the limiting global density of the known Jacobi ensemble [24, 25] diverges like a square root at the endpoints ± 1, we expect hard edge behaviour at our edge points. For the chiral ensemble [19] the scaling of weak non-Hermiticity in N also agrees with the bulk scaling [11], which is consistent with our findings. Notice that for any $\tau < 1$ the foci of our ellipse (2.2) are located at ± 1 in the interior of the ellipse.

Let us emphasise that our bulk limit is special though, as in this limit the edges of the ellipse become close to the real interval $(-1, 1)$. Thus our bulk points become squeezed between these edges, representing hard walls, in the vicinity of the interval. For that reason we may expect that our bulk limit differs from the bulk limit of the Ginibre ensemble. Only when the bulk becomes broader again we recover the Ginibre result, see section 4.1.

The weak non-Hermiticity limit both in the bulk and at the edge of the spectrum is defined by taking the limit $\tau \to 1$ such that

$$\frac{1}{\tau} = 1 + \frac{s^2}{2N^2}, \quad 0 < s < \infty, \tag{4.1}$$

with $N \to \infty$, and the weak non-Hermiticity parameter s is kept fixed[6]. For later use we collect the following expressions

$$\tau = \frac{1}{1 + \frac{s^2}{2N^2}}, \quad \frac{\tau}{1-\tau} = \frac{2N^2}{s^2}, \quad \frac{\tau}{1+\tau} = \frac{2N^2}{4N^2 + s^2}. \tag{4.2}$$

Given that the Gegenbauer polynomials can be expressed in terms of the Jacobi polynomials, e.g. in (3.17), it turns out that in both the bulk and edge limits the following asymptotic form of the general Jacobi polynomials $P^{(\alpha,\gamma)}(z)$ will be useful, [31, 18.11.5]:

$$P_n^{(\alpha,\gamma)}\left(1 - \frac{Z}{2n^2}\right) \sim n^\alpha \left(\frac{\sqrt{Z}}{2}\right)^{-\alpha} J_\alpha\left(\sqrt{Z}\right), \quad n \to \infty, \tag{4.3}$$

with fixed real α and γ, and $Z = X + \mathrm{i}Y$ (X and Y are real) kept fixed. Recall that the polynomials $P^{(\alpha,\gamma)}(x)$ are orthogonal with respect to the weight $(1-x)^\alpha(1+x)^\gamma$ on $[-1, 1]$, and satisfy the following reflection symmetry:

$$P_n^{(\alpha,\gamma)}(-z) = (-1)^n P_n^{(\gamma,\alpha)}(z), \tag{4.4}$$

and that the asymptotic form (4.3) zooming into the vicinity of $+1$ is independent of γ.

4.1. Weak non-Hermiticity in the bulk

In this subsection we consider the bulk scaling limit in the vicinity of the origin, by rescaling the complex variables inside the kernel (3.11) as

$$z_j = x_j + iy_j = \frac{\hat{z}_j}{N}, \quad j = 1, 2, \tag{4.5}$$

where $\hat{z}_j = \hat{x}_j + \mathrm{i}\hat{y}_j$ ($\hat{x}_j$ and $\hat{y}_j$ are real) are kept fixed when $N \to \infty$. We expect that the limiting kernel, after some suitable modification, does not depend on the location in the bulk, and we will check this conjecture with a consistency check in the next section 4.2.

[6] Note that in [11] this parameter is typically found to be proportional to $(1-\tau)N$.

As a short calculation for the scaling limit (given by (4.1) and (4.5)) of the pre-factors of the kernel in the first line of (3.11), that originate from the weight function, we obtain

$$\lim_{N\to\infty}\left(1-\frac{2\tau}{1+\tau}x_j^2-\frac{2\tau}{1-\tau}y_j^2\right)^{a/2}=\left(1-4\frac{\hat{y}_j^2}{s^2}\right)^{a/2}, \tag{4.6}$$

for $j=1,2$. Here, only the imaginary part of the scaling variable $\hat{z}_j=\hat{x}_j+\mathrm{i}\hat{y}_j$ appears. From this limit we can read off the domain of the scaling variables $\hat{z}_j$ ($j=1,2$) in the bulk limit:

$$D_{\mathrm{Bulk}}=\left\{\hat{z}\,\middle|\,\frac{s^2}{4}\geqslant\hat{y}^2\ \text{ and }\ -\infty<\hat{x}<\infty\right\}, \tag{4.7}$$

with $\hat{z}=\hat{x}+\mathrm{i}\hat{y}$ ($\hat{x}$ and $\hat{y}$ are real).

In the kernel (3.11) the sum will turn into an integral. Because we split the sum into its even and odd parts, let us present the details of this step. For f_n some continuous and integrable function depending on n we have

$$\begin{aligned}\sum_{n=0}^{N-1}(n+a+1)f_n&=\sum_{\ell=0}^{\lfloor\frac{N-1}{2}\rfloor}(2\ell+a+1)f_{2\ell}+\sum_{\ell=0}^{\lfloor\frac{N-2}{2}\rfloor}(2\ell+a+2)f_{2\ell+1}\\&\sim\frac{N^2}{2}\int_0^1\mathrm{d}c\,c\left(f\left(\frac{2\ell}{N}=c\right)+f\left(\frac{2\ell+1}{N}=c\right)\right),\end{aligned} \tag{4.8}$$

in the limit $N\to\infty$, where $\ell=\lfloor n/2\rfloor$. We also introduced the integration variable

$$c=\frac{n}{N}=\frac{2\ell}{N}\ \text{or}\ \frac{2\ell+1}{N}\in[0,1], \tag{4.9}$$

and use that

$$\frac{2}{N}\sum_{\ell=0}^{\mathcal{L}}\to\int_0^1\mathrm{d}c,\quad\text{for }\mathcal{L}=\left\lfloor\frac{N-1}{2}\right\rfloor\ \text{or}\ \left\lfloor\frac{N-2}{2}\right\rfloor. \tag{4.10}$$

For the asymptotic form of the Gegenbauer polynomials inside the sum of (3.11), we can apply the asymptotic form of the Jacobi polynomials (4.3). As we zoom into the origin with small argument of the Gegenbauer polynomials (4.5), while the asymptotic (4.3) is in the vicinity of the endpoint, we cannot use the standard mapping (3.17) of the Gegenbauer polynomials to the symmetric Jacobi polynomials. Fortunately a different map exists, and we begin with the even Gegenbauer polynomials. Using [31, 18.7.15], we have

$$\begin{aligned}C_{2\ell}^{(a+1)}(x)&=\frac{(a+1)_\ell}{(1/2)_\ell}P_\ell^{(a+\frac12,\,-\frac12)}(2x^2-1)\\&=\frac{\Gamma(\ell+a+1)\,\Gamma(1/2)}{\Gamma(a+1)\,\Gamma\left(\ell+\frac12\right)}(-1)^\ell P_\ell^{(-\frac12,\,a+\frac12)}(1-2x^2),\end{aligned} \tag{4.11}$$

where $(b)_n = \Gamma(b+n)/\Gamma(b)$ is the Pochhammer symbol. From (4.3) we thus obtain

$$\begin{aligned}\lim_{N\to\infty}\frac{1}{N^a}(-1)^\ell C_{2\ell}^{(a+1)}\left(\frac{\hat{z}}{N}\right) &= \frac{\sqrt{\pi}c^a}{2^a\Gamma(a+1)}\lim_{N\to\infty}\ell^{\frac{1}{2}}P_\ell^{(-\frac{1}{2},\,a+\frac{1}{2})}\left(1-2\frac{\hat{z}^2}{N^2}\right)\\ &= \frac{\sqrt{\pi}c^a}{2^a\Gamma(a+1)}\left(\frac{c\hat{z}}{2}\right)^{\frac{1}{2}}J_{-\frac{1}{2}}(c\hat{z})\\ &= \frac{c^a}{2^a\Gamma(a+1)}\cos(c\hat{z}).\end{aligned} \tag{4.12}$$

Here, $c = 2\ell/N$ is fixed in the limit $N \to \infty$, and in the last step we have used [32, 8.464.2]

$$J_{-\frac{1}{2}}(z) = \sqrt{\frac{2}{\pi z}}\cos(z). \tag{4.13}$$

The very same steps can be taken for the asymptotic form of the odd Gegenbauer polynomials. Using [31, 18.7.16], we start from the map

$$\begin{aligned}C_{2\ell+1}^{(a+1)}(x) &= \frac{(a+1)_{\ell+1}}{(1/2)_{\ell+1}}xP_\ell^{(a+\frac{1}{2},\,\frac{1}{2})}(2x^2-1)\\ &= \frac{\Gamma(\ell+a+2)\,\Gamma(1/2)}{\Gamma(a+1)\,\Gamma\left(\ell+\dfrac{3}{2}\right)}(-1)^\ell xP_\ell^{(\frac{1}{2},\,a+\frac{1}{2})}(1-2x^2).\end{aligned} \tag{4.14}$$

Once again (4.3) leads to

$$\begin{aligned}\lim_{N\to\infty}\frac{1}{N^a}(-1)^\ell C_{2\ell+1}^{(a+1)}\left(\frac{\hat{z}}{N}\right) &= \frac{\sqrt{\pi}c^a}{2^a\Gamma(a+1)}\lim_{N\to\infty}\frac{\hat{z}}{N}\ell^{\frac{1}{2}}P_\ell^{(\frac{1}{2},\,a+\frac{1}{2})}\left(1-2\frac{\hat{z}^2}{N^2}\right)\\ &= \frac{\sqrt{\pi}c^a}{2^a\Gamma(a+1)}\left(\frac{c\hat{z}}{2}\right)^{\frac{1}{2}}J_{\frac{1}{2}}(c\hat{z})\\ &= \frac{c^a}{2^a\Gamma(a+1)}\sin(c\hat{z}).\end{aligned} \tag{4.15}$$

Here, $c = (2\ell+1)/N$ is fixed in the limit $N \to \infty$, and in the last step we have used [32, 8.464.1]

$$J_{\frac{1}{2}}(z) = \sqrt{\frac{2}{\pi z}}\sin(z). \tag{4.16}$$

For the Gegenbauer polynomials from the normalisation in the denominator inside the sum of (3.11), the argument is $1/\tau$. Using (4.1), we see that we can directly use (4.3) together with the standard map (3.17), valid for both even and odd polynomials alike. By analytic continuation of the asymptotic (4.3) to imaginary argument, $Z \to iZ$, we obtain for the normalising Gegenbauer polynomial of the scaling variable (4.1)

$$\lim_{n\to\infty}\frac{1}{N^{2a+1}}C_n^{(a+1)}\left(1+\frac{s^2}{2N^2}\right) = \frac{\Gamma\left(a+\frac{3}{2}\right)}{\Gamma(2a+2)}\left(\frac{2}{cs}\right)^{a+\frac{1}{2}}I_{a+\frac{1}{2}}(cs), \tag{4.17}$$

with $c = n/N$ fixed. Here, $I_\alpha(z)$ is the modified Bessel function of the first kind.

Putting all the above together we obtain the following result for the bulk scaling limit of the kernel (3.11) around the origin:

$$
\begin{aligned}
K_{\mathrm{Bulk}}(\hat{z}_1,\hat{z}_2) &= \lim_{N\to\infty}\frac{1}{N^2}K_N\left(\frac{\hat{z}_1}{N},\frac{\hat{z}_2}{N}\right)\\
&= \left(1-\frac{4\hat{y}_1^2}{s^2}\right)^{\frac{a}{2}}\left(1-\frac{4\hat{y}_2^2}{s^2}\right)^{\frac{a}{2}}\frac{1}{\pi s}\frac{s^{a+\frac{1}{2}}\Gamma(2a+2)}{2^{3a+\frac{1}{2}}\Gamma\left(a+\frac{3}{2}\right)\Gamma(a+1)^2}\\
&\quad\times\int_0^1 \mathrm{d}c\,\frac{c^{a+\frac{1}{2}}\left(\cos(c\hat{z}_1)\cos(c\bar{\hat{z}}_2)+\sin(c\hat{z}_1)\sin(c\bar{\hat{z}}_2)\right)}{I_{a+\frac{1}{2}}(cs)}\\
&= \frac{2}{s\pi^{\frac{3}{2}}\Gamma(a+1)}\left(1-\frac{4\hat{y}_1^2}{s^2}\right)^{\frac{a}{2}}\left(1-\frac{4\hat{y}_2^2}{s^2}\right)^{\frac{a}{2}}\int_0^1 \mathrm{d}c\,\frac{(cs/2)^{a+\frac{1}{2}}}{I_{a+\frac{1}{2}}(cs)}\cos(c(\hat{z}_1-\bar{\hat{z}}_2)).
\end{aligned}
\tag{4.18}
$$

In the second step we have used an addition theorem for the trigonometric functions and (3.20).

The corresponding microscopic level density only depends on the imaginary part, see (4.18), and reads

$$
\varrho(\hat{y}) = K_{\mathrm{Bulk}}(\hat{x}+\mathrm{i}\hat{y},\hat{x}+\mathrm{i}\hat{y}). \tag{4.19}
$$

In figure 4 we illustrate the effects of the parameters a and s. While an increasing non-Hermiticity s presses the spectrum away from the real axis to the boundary, see figure 4(a), a growing a results in the opposite effect, see, figure 4(b). The parameter a represents the charge of the hard wall of the boundary of the ellipse leading to a repulsion of the particles from the boundary. When both parameters grow large and one zooms into the real axis we find the translation invariant bulk statistics of the Ginibre ensemble, see figure 4(c).

The limiting kernel (4.18) is a deformation of the sine-kernel in the complex plane. It holds inside the domain (4.7), where the two pre-factors originating from the weight have non-negative arguments. We conjecture that the same limiting kernel is found, when we zoom into any point $x_0 \in (-1, 1)$, and make a bulk scaling limit there, with an appropriate shift of the weight and rescalings. This conjecture is supported by the fact that a similar asymptotic form (4.52) holds in the vicinity of the edge, as the bulk limit of the edge kernel.

We note here that—in addition to the pre-factors stemming from the weight function—the deformed sine-kernel in the bulk scaling limit at the origin (4.18) also differs inside the integral from what is obtained as a deformed sine-kernel in the weak non-Hermiticity limit of the elliptic Ginibre ensemble [11], see [21, equation (2.22)] for a comparison in that form. There, the pre-factor multiplying cosine is replaced by a simple exponential. This difference remains valid for any fixed value of $a > -1$ as well as for large arguments, as we will see below.

In the following we will take two limits of the bulk kernel (4.18) in order to compare to other known results. We begin with the Hermitian limit as a consistency check.

(1) *The Hermitian limit $s \to 0$:*

In this limit the local bulk kernel is mapped back to the real axis. This can be seen from the support (4.7) of length s in $\hat{y}$-direction shrinking to zero, leading to $\hat{y}_1, \hat{y}_2 \to 0$ in (4.18). For the denominator of the integrand we have the small argument asymptotic relation of the modified Bessel-function, see e.g. in [32, 8.445]

$$
I_{a+\frac{1}{2}}(cs) \sim \frac{(cs/2)^{a+\frac{1}{2}}}{\Gamma\left(a+\frac{3}{2}\right)}, \quad s \to 0. \tag{4.20}
$$

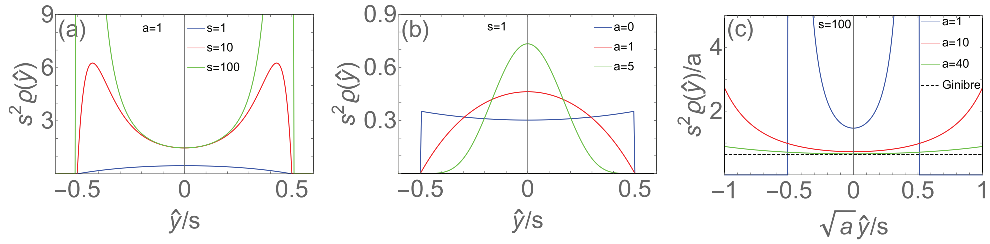

Figure 4. Microscopic level density (4.19) as a function of the imaginary part $\hat{y}$ for various charges a of the ellipses boundary and for various values of the non-Hermiticity parameter s. In the plot (a) with $a = 1$ and plot (b) with $s = 1$ fixed we employ the scaling of the strong non-Hermiticity limit with the domain (4.22), hence, the fixed support of $\hat{y}$ is the interval $[-1/2, 1/2]$. In contrast, we want to illustrate the limit to the Ginibre result (dashed straight line on the height $2/\pi$) in the plot (c). Therefore, here the size of the support grows with $\sqrt{a}$.

Before taking the limit $s \to 0$ we have to recall that the ellipse E and $[-1, 1]$ are normalised differently, see (3.10) and (3.16). Because from (4.2) we can read off the constant $A \sim \dfrac{1}{N}\dfrac{s\pi}{2(a+1)}$, we propose to take the following normalised Hermitian limit

$$\begin{aligned}
\lim_{s\to 0} \frac{s\pi}{2(a+1)B} K_{\mathrm{Bulk}}(\hat{z}_1, \hat{z}_2)\bigg|_{\hat{y}_1=\hat{y}_2=0} &= \frac{\pi}{2(a+1)B} \frac{2\Gamma\left(a+\frac{3}{2}\right)}{\pi^{\frac{3}{2}}\Gamma(a+1)} \int_0^1 \mathrm{d}c \cos(c(\hat{x}_1 - \hat{x}_2)) \\
&= \frac{1}{\pi} \frac{\sin(\hat{x}_1 - \hat{x}_2)}{\hat{x}_1 - \hat{x}_2} .
\end{aligned} \tag{4.21}$$

It results into the well-known universal sine-kernel. It is known to hold for the Jacobi ensemble in the bulk of the spectrum [24], as well as for other ensembles.

(2) *The strong non-Hermiticity limit $s \to \infty$:*
This limit is expected to reproduce the limiting kernel at strong non-Hermiticity, when rescaling $\tilde{z}_j = \tilde{x}_j + \mathrm{i}\tilde{y}_j = \hat{z}_j/s$ for $j = 1, 2$ ($\tilde{x}_j$ and $\tilde{y}_j$ are real). The same mechanism was applied in the elliptic Ginibre ensemble in [11]. The corresponding domain (4.7) gets mapped to

$$D_{\mathrm{Bulk,\ strong}} = \left\{ \tilde{z} \,\middle|\, \frac{1}{4} \geqslant \tilde{y}^2 \ \text{ and } \ -\infty < \tilde{x} < \infty \right\}, \tag{4.22}$$

with $\tilde{z} = \tilde{x} + \mathrm{i}\tilde{y}$ ($\tilde{x}$ and $\tilde{y}$ are real). It is an infinite strip of unit width parallel to the $\tilde{x}$-axis. We obtain the following expression for the limit of the integral in (4.18):

$$\begin{aligned}
\mathcal{J}_a &= \lim_{s\to\infty} s \int_0^1 \mathrm{d}c \frac{(cs/2)^{a+\frac{1}{2}}}{I_{a+\frac{1}{2}}(cs)} \cos(c(\hat{z}_1 - \bar{\hat{z}}_2)) \\
&= \lim_{s\to\infty} \int_0^s \mathrm{d}t \frac{(t/2)^{a+\frac{1}{2}}}{I_{a+\frac{1}{2}}(t)} \cos(t(\tilde{z}_1 - \bar{\tilde{z}}_2)) \\
&= \int_0^\infty \mathrm{d}t \frac{(t/2)^{a+\frac{1}{2}}}{I_{a+\frac{1}{2}}(t)} \cos(t(\tilde{z}_1 - \bar{\tilde{z}}_2)).
\end{aligned} \tag{4.23}$$

Here we have changed the integration variable to $t = cs$. The final answer for the limiting kernel at strong non-Hermiticity on the domain (4.22) thus reads

$$\begin{aligned} K_{\text{Bulk,strong}}(\tilde{z}_1, \tilde{z}_2) &= \lim_{s\to\infty} s^2 K_{\text{Bulk}}(s\tilde{z}_1, s\tilde{z}_2) \\ &= \frac{2}{\pi^{\frac{3}{2}}\Gamma(a+1)} \left(1-4\tilde{y}_1^2\right)^{\frac{a}{2}} \left(1-4\tilde{y}_2^2\right)^{\frac{a}{2}} \int_0^\infty \mathrm{d}t \frac{(t/2)^{a+\frac{1}{2}}}{I_{a+\frac{1}{2}}(t)} \cos(t(\tilde{z}_1 - \bar{\tilde{z}}_2)). \end{aligned} \tag{4.24}$$

Although we have derived the kernel (4.24) indirectly via the weak non-Hermiticity limit at the origin, we conjecture it to be universal, after an appropriate shift of the weight away from the origin plus rescalings. Because the appropriate Mehler or Poisson formula for the kernel (3.11) is lacking, when extending the sum to infinity[7], we have been unable to directly take the strong non-Hermiticity limit.

Notice that the kernel (4.24) does not agree with the Ginibre kernel in the bulk of the spectrum of the elliptic Ginibre ensemble. In oder to recover the Ginibre kernel, we need to take the limit $a \to \infty$ with a suitable scaling, as explained below. Furthermore, yet another limiting kernel exists, which is obtained when imposing a hard edge (at the otherwise soft edge) for the Ginibre ensemble, see [6, theorem 2.3]. Apparently the role of a hard edge differs when imposed for a confining potential as for Ginibre, or for a non-confining potential as here, generalising the Jacobi ensemble.

Let us explain how to recover the Ginibre kernel in the limit $a \to \infty$. A series expansion [31, 10.25.2]

$$I_{a+\frac{1}{2}}(t) = \left(\frac{t}{2}\right)^{a+\frac{1}{2}} \sum_{\ell=0}^{\infty} \frac{(t^2/4)^\ell}{\ell!\,\Gamma\left(\ell+a+\frac{3}{2}\right)} \tag{4.25}$$

is known for the modified Bessel function. Introducing a new variable $\hat{t} = t/\sqrt{a}$ and using the asymptotic relation

$$\frac{\Gamma\left(a+\frac{3}{2}\right)}{\Gamma\left(\ell+a+\frac{3}{2}\right)} \sim a^{-\ell}, \quad a\to\infty, \tag{4.26}$$

for a fixed non-negative integer ℓ, we obtain

$$I_{a+\frac{1}{2}}(\sqrt{a}\hat{t}) \sim \left(\frac{\sqrt{a}\hat{t}}{2}\right)^{a+\frac{1}{2}} \frac{\mathrm{e}^{\hat{t}^2/4}}{\Gamma\left(a+\frac{3}{2}\right)}, \quad a\to\infty, \tag{4.27}$$

from (4.25). Here $\hat{t}$ is fixed. We put this asymptotic form into (4.23) and find

$$\begin{aligned} \mathcal{J}_a &= \sqrt{a}\int_0^\infty \mathrm{d}\hat{t} \frac{(\sqrt{a}\hat{t}/2)^{a+\frac{1}{2}}}{I_{a+\frac{1}{2}}(\sqrt{a}\hat{t})} \cos(\sqrt{a}\hat{t}(\tilde{z}_1 - \bar{\tilde{z}}_2)) \\ &\sim \sqrt{a}\,\Gamma\left(a+\frac{3}{2}\right) \int_0^\infty \mathrm{d}\hat{t}\, \mathrm{e}^{-\hat{t}^2/4} \cos\left(\hat{t}(u_1 - \bar{u}_2)\right) \\ &= \sqrt{\pi a}\,\Gamma\left(a+\frac{3}{2}\right) \mathrm{e}^{-(u_1-\bar{u}_2)^2}, \end{aligned} \tag{4.28}$$

[7] Notice that a different Poisson kernel exists for the general Jacobi polynomials, see [33].

where $u_j = \sqrt{a}\tilde{z}_j$ $(j = 1, 2)$. Then it follows that

$$\widetilde{K}_{\rm Ginibre}(u_1, u_2) = \lim_{a\to\infty} K_{\rm Bulk,\ strong}\left(u_1/\sqrt{a}, u_2/\sqrt{a}\right)/a$$
$$= \frac{2}{\pi}\exp\left[-|u_1|^2 - |u_2|^2 + 2u_1\bar{u}_2 - {\rm i}\Im(u_1^2 - u_2^2)\right]. \tag{4.29}$$

This kernel is equivalent[8] to the Ginibre kernel $K_{\rm Ginibre}(u_1, u_2)$, presented below.

Though the Ginibre kernel was originally found in [1] for the Gaussian random matrix model (with the kernel (3.27) in the limit $\tau \to 0$), it can also be derived from truncated unitary random matrices [18]. Starting from the kernel function (3.14) of truncated unitary random matrices, one can take the aymptotic limit $N \to \infty$ and obtains

$$K^{\rm truncated}(z_1, z_2) = \lim_{N\to\infty} K_N^{\rm truncated}(z_1, z_2)$$
$$= (1 - |z_1|^2)^{\frac{a}{2}}(1 - |z_2|^2)^{\frac{a}{2}}\sum_{n=0}^{\infty}\frac{\Gamma(n + a + 2)}{\pi\Gamma(a + 1)\Gamma(n + 1)}(z_1\bar{z}_2)^n$$
$$= \frac{a + 1}{\pi}\frac{(1 - |z_1|^2)^{\frac{a}{2}}(1 - |z_2|^2)^{\frac{a}{2}}}{(1 - z_1\bar{z}_2)^{a+2}}, \tag{4.30}$$

for fixed z_1 and z_2 satisfying $|z_1| < 1$ and $|z_2| < 1$. Introducing variables $u_j = \sqrt{\frac{a}{2}}z_j$ $(j = 1, 2)$ and taking the limit $a \to \infty$, one arrives at the Ginibre kernel

$$K_{\rm Ginibre}(u_1, u_2) = \lim_{a\to\infty} K^{\rm truncated}\left(u_1/\sqrt{a/2},\ u_2/\sqrt{a/2}\right)/(a/2)$$
$$= \frac{2}{\pi}\exp\left(-|u_1|^2 - |u_2|^2 + 2u_1\bar{u}_2\right). \tag{4.31}$$

4.2. Weak non-Hermiticity at the edge

In this subsection we consider the weak non-Hermiticity limit at the edge of the spectrum. Because the Gegenbauer polynomials have parity, without loss of generality we magnify the region around the focus at $+1$, in choosing the scaling

$$z_j = 1 - \frac{Z_j}{2N^2}, \quad j = 1, 2, \tag{4.32}$$

together with the weak non-Hermiticity limit (4.1). Here, the complex numbers $Z_j = X_j + {\rm i}Y_j$ are fixed (X_j and Y_j are real). In this limit the pre-factors of the kernel (3.11) from the weight turn into

$$\left(1 - \frac{2\tau}{1 + \tau}x_j^2 - \frac{2\tau}{1 - \tau}y_j^2\right)^{a/2} \sim N^{-a}\left(\frac{s^2}{4} + X_j - \left(\frac{Y_j}{s}\right)^2\right)^{a/2}, \tag{4.33}$$

in the limit $N \to \infty$ as (4.1) and (4.32). Once again we keep the parameter a fixed in this limit. Equation (4.33) implies that the limiting domain of the scaled particle positions (X_j, Y_j) becomes the parabolic domain

[8] Two kernels are equivalent if they agree up to multiplication by $f(u_1)/f(u_2)$ as they yield the same correlation functions in (3.3), with $f(u_1) = {\rm e}^{-{\rm i}\Im u_1^2}$ here.

$$D_{\text{Edge}} = \left\{ (X, Y) \middle| X \geqslant \left(\frac{Y}{s}\right)^2 - \frac{s^2}{4} \right\}, \tag{4.34}$$

which is a magnified part around the right focus of the ellipse, that is the right endpoint of $[-1, 1]$.

The pre-factor of the sum in the second line of (3.11) is easily evaluated by using (4.2), to give

$$\frac{2\tau}{\pi\sqrt{1-\tau^2}} = \frac{2}{\pi}\sqrt{\frac{\tau}{1-\tau}\frac{\tau}{1+\tau}} \sim \frac{2N}{s\pi}. \tag{4.35}$$

Due to the relation (3.17) of the Gegenbauer polynomials to the symmetric Jacobi polynomials, and their asymptotic form (4.3) in the vicinity of unity, we find the following asymptotic relation,

$$C_n^{(a+1)}(z_j) = C_n^{(a+1)}\left(1 - \frac{Z_j}{2N^2}\right) \sim N^{2a+1}\frac{\Gamma\left(a+\frac{3}{2}\right)}{\Gamma(2a+2)}\left(\frac{\sqrt{Z_j}}{2c}\right)^{-a-\frac{1}{2}} J_{a+\frac{1}{2}}\left(c\sqrt{Z_j}\right). \tag{4.36}$$

Because the limit of the squared norms does not depend on the point we magnify, we may use again the asymptotic (4.17) from the previous subsection.

Inserting (4.33), (4.35), (4.36) and (4.17) together in (3.11), and replacing the sum by an integral, yields the following asymptotic formula for the limiting kernel at the edge

$$\begin{aligned} K_{\text{Edge}}(Z_1, Z_2) &= \lim_{N\to\infty}\frac{1}{4N^4}K_N(z_1, z_2) \\ &= \frac{1}{4\sqrt{\pi}\Gamma(a+1)}\left(\frac{s}{2}\right)^{a-\frac{1}{2}}\left(\frac{s^2}{4} + X_1 - \left(\frac{Y_1}{s}\right)^2\right)^{\frac{a}{2}}\left(\frac{s^2}{4} + X_2 - \left(\frac{Y_2}{s}\right)^2\right)^{\frac{a}{2}} \\ &\quad\times\left(\sqrt{Z_1\bar{Z}_2}\right)^{-a-\frac{1}{2}}\int_0^1 \mathrm{d}c\,\frac{c^{a+\frac{3}{2}}}{I_{a+\frac{1}{2}}(cs)}J_{a+\frac{1}{2}}\left(c\sqrt{Z_1}\right)J_{a+\frac{1}{2}}\left(c\sqrt{\bar{Z}_2}\right), \end{aligned} \tag{4.37}$$

with a fixed $a > -1$. This limiting kernel is a deformation of the Bessel-kernel into the complex plane, holding inside the domain (4.34) where the two pre-factors from the weight have non-negative arguments. From symmetry the same limiting kernel is obtained at the left edge of the ellipse. Not only the pre-factors from the weight but also the pre-factor in the integrand inversely proportional to the modified I-Bessel function differs from the pre-factor of the deformed Bessel-kernel of the chiral ensemble [19], given by an exponential. There, $a + \frac{1}{2} = \nu$, and for integer values it corresponds to the number of zero-modes therein. This difference remains valid for any fixed values $a > -1$, and shows the influence of the boundary. It pertains also for large arguments, as we will see below. We expect that the limiting edge-kernel (4.37) is also universal.

Again we define a microscopic density which depends this time on both the real and imaginary parts, due to the loss of translation invariance, i.e.

$$\hat{\varrho}(X, Y) = K_{\text{Edge}}(X + \mathrm{i}Y, X + \mathrm{i}Y). \tag{4.38}$$

Its dependence on an increasing non-Hermiticity s and an increasing charge a is illustrated in figures 5 and 6, respectively. Note that the positive direction of the horizontal axis is the direction to the left to reflect the position of the edge where we zoom into the spectrum. At the edge we have a similar picture compared to the microscopic bulk regime. The spectrum lies in

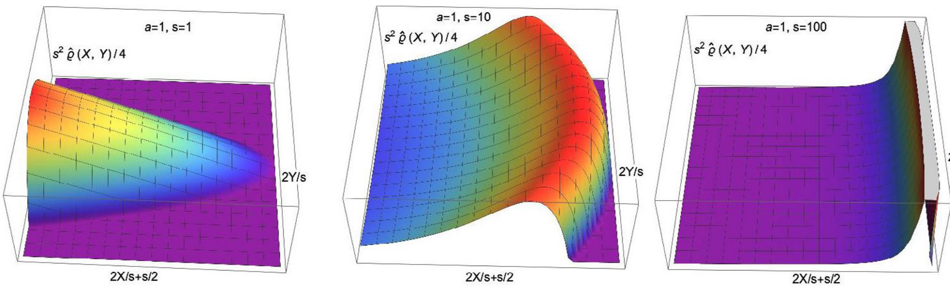

Figure 5. The rescaled microscopic level density (4.38) $s^2\hat{\varrho}(X,Y)/4$ at the edge for increasing non-Hermiticity $s = 1\,10\,100$ (from left to right) at fixed charge $a = 1$ of the boundary. The color coding of the graph highlights the height of the function. The scaling of the real and imaginary parts are those of the strong non-Hermiticity limit, see (4.40).

a constant competition between s, which tries to spread and squeeze it into the boundary, and a, which creates a repulsion from exactly the same boundary.

Below we will take two limits of the kernel (4.37) to compare with known asymptotic kernels in random matrix theory, the Hermitian and strong non-Hermiticity limit. In addition we take a third limit of large argument, that brings us back to the result in the bulk from the previous subsection.

(1) *The Hermitian limit $s \to 0$:*
In this limit, we can see from the domain (4.34) that it requires $Y_j = 0$, and the real parts are confined to the half line, $X_j \geqslant 0$. For the normalisation of this Hermitian limit we follow (4.21), and for the pre-factor inside the integral in (4.37) we may use again the asymptotic (4.20). This leads to the following result:

$$\lim_{s\to 0} \frac{s\pi}{2(a+1)B} K_{\text{Edge}}(Z_1, Z_2)\Big|_{X_{1,2}\geqslant 0,\ Y_{1,2}=0}$$
$$= \frac{1}{4}(X_1X_2)^{-\frac{1}{4}} \int_0^1 \mathrm{d}c\, c\, J_{a+\frac{1}{2}}\left(c\sqrt{X_1}\right) J_{a+\frac{1}{2}}\left(c\sqrt{X_2}\right), \tag{4.39}$$

with a fixed $a > -1$. This reproduces a well-known universal result, the Bessel-kernel, derived for the symmetric Jacobi ensemble of random Hermitian matrices [25] with weight (2.10). Note that the non-constant pre-factor $(X_1X_2)^{-1/4}$ is cancelled in the expressions of the correlation functions, when we make variable transformations $X_j \mapsto X_j^2$.

(2) *The strong non-Hermiticity limit $s \to \infty$:*
Let us next consider the opposite limit $s \to \infty$, to obtain the limiting kernel at strong non-Hermiticity. For that purpose, we introduce new scaling variables

$$\tilde{X}_j = \frac{2}{s}X_j + \frac{s}{2}, \quad \tilde{Y}_j = \frac{2}{s}Y_j, \tag{4.40}$$

where we keep $\tilde{X}_j$ and $\tilde{Y}_j$ fixed when taking the limit $s \to \infty$. In terms of these new variables the determining equation for the domain (4.34) becomes $\frac{s}{2}\tilde{X}_j \geqslant \frac{\tilde{Y}_j^2}{4}$. Thus in the limit the scaled particle positions $(\tilde{X}_j, \tilde{Y}_j)$ are confined to the half plane, that is $0 \leqslant \tilde{X}_j < \infty$ and $-\infty < \tilde{Y}_j < \infty$. Now we use the asymptotic formula [28] for $u \to \infty$,

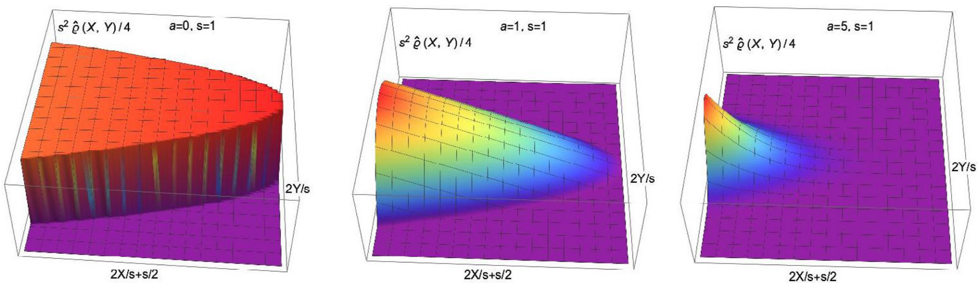

Figure 6. The rescaled microscopic level density (4.38) $s^2\hat{\varrho}(X,Y)/4$ at the edge for increasing charge $a=0,1,5$ (from left to right) at fixed non-Hermiticity $s=1$. Again we have employed the scaling (4.40), see also figure 5.

$$J_b\left(uz\right)\sim\left(\frac{2}{\pi uz}\right)^{1/2}\cos\left(uz-\frac{\pi}{2}b-\frac{\pi}{4}\right),\tag{4.41}$$

for a fixed real index b and a fixed complex z, to obtain

$$\left(\sqrt{Z_j}\right)^{-a-\frac{1}{2}}J_{a+\frac{1}{2}}\left(c\sqrt{Z_j}\right)\sim\left(\frac{s}{2}\right)^{-a-\frac{1}{2}}(\pi cs)^{-1/2}\exp\left[\frac{cs}{2}\left(1-\frac{1}{s}\left(\tilde{X}_j+\mathrm{i}\tilde{Y}_j\right)\right)\right],\tag{4.42}$$

for $s\to\infty$. Together with the large-s asymptotic for the modified Bessel functions, see [32, 8.451.5],

$$I_{a+\frac{1}{2}}\left(cs\right)\sim\left(2\pi cs\right)^{-1/2}\mathrm{e}^{cs},\quad s\to\infty,\tag{4.43}$$

valid for any fixed a, it then follows for the scaling (4.40) that

$$\begin{aligned}K_{\mathrm{Edge,strong}}(\tilde{Z}_1,\tilde{Z}_2)&=\lim_{s\to\infty}\frac{s^2}{4}K_{\mathrm{Edge}}(Z_1,Z_2)\\&=\frac{(\tilde{X}_1\tilde{X}_2)^{a/2}}{4\pi\Gamma(a+1)}\int_0^1\mathrm{d}c\,c^{a+1}\exp\left[-\frac{c}{2}(\tilde{X}_1+\tilde{X}_2)-\mathrm{i}\frac{c}{2}(\tilde{Y}_1-\tilde{Y}_2)\right],\end{aligned}\tag{4.44}$$

with a fixed $a>-1$. This limiting kernel is not new and, as we will show below, agrees with the kernel found for truncated unitary matrices [18] in what the authors call weakly non-unitary limit. What we call strongly non-Hermitian here is to be understood in the sense that by taking the limit $s\to\infty$ we reestablish rotational invariance.

Starting directly from the kernel of the truncated unitary matrix ensemble (3.14), we may introduce scaled real variables $\hat{X}_j$ and $\hat{Y}_j$ that remain fixed when $N\to\infty$,

$$z_j=1-\frac{\hat{X}_j}{2N}-\mathrm{i}\frac{\hat{Y}_j}{2N},\tag{4.45}$$

magnifying the edge region of the unit circle at unity. Then, we obtain

$$\lim_{N\to\infty}\frac{1}{4N^2}K_N^{\mathrm{truncated}}(z_1,z_2)=\frac{\left(\hat{X}_1\hat{X}_2\right)^{a/2}}{4\pi\Gamma(a+1)}\int_0^1\mathrm{d}c\,c^{a+1}\exp\left[-\frac{c}{2}(\hat{X}_1+\hat{X}_2)-\mathrm{i}\frac{c}{2}(\hat{Y}_1-\hat{Y}_2)\right].\tag{4.46}$$

It is in agreement with the asymptotic formula (4.44), and the scaled density $\rho(\tilde{Z}_1)=K_{\mathrm{Edge,strong}}(\tilde{Z}_1,\tilde{Z}_1)$ agrees with the density computed in [18, equation (21)].

(3) *The bulk limit:*

It is known that, in taking the large argument limit, the correlations at the edge get mapped back to the correlations in the bulk, see e.g. [34]. Thus this limit will allow us to check our conjecture that a similar asymptotic form to the kernel (4.18) is valid in the entire bulk. Let us therefore introduce scaled complex variables $\hat{z}_j = \hat{x}_j + i\hat{y}_j$ for the arguments of the edge kernel (4.37) as

$$Z_j = \kappa h - 2\sqrt{h}\hat{z}_j, \tag{4.47}$$

where $\kappa > 0$ and $\hat{z}_j$ remain fixed, and we will take the limit of h positive to become large, $h \to \infty$. In these variables the defining equation for the domain (4.34) with $Z = X + iY = \kappa h - 2\sqrt{h}\hat{z}$ becomes

$$\kappa h - 2\sqrt{h}\hat{x} \geqslant \frac{4h\hat{y}^2}{s^2} - \frac{s^2}{4}, \tag{4.48}$$

leading to the domain

$$D_{\mathrm{Bulk}} = \left\{ \hat{z} \,\middle|\, \frac{s^2}{4}\kappa \geqslant \hat{y}^2 \quad \text{and} \quad -\infty < \hat{x} < \infty \right\}, \tag{4.49}$$

where $\hat{z} = \hat{x} + i\hat{y}$.

For the scaling (4.47) we can readily see that

$$\sqrt{Z_j} \sim \sqrt{\kappa h} - \frac{\hat{z}_j}{\sqrt{\kappa}}, \quad h \to \infty. \tag{4.50}$$

Then, we can utilize (4.41) to find that

$$J_{a+\frac{1}{2}}\left(c\sqrt{Z_j}\right) \sim \left(\frac{2}{c\pi\sqrt{\kappa h}}\right)^{1/2} \cos\left(c\sqrt{\kappa h} - \frac{c\hat{z}_j}{\sqrt{\kappa}} - \frac{\pi}{2}a - \frac{\pi}{2}\right), \quad h \to \infty. \tag{4.51}$$

Putting the above asymptotic results for the scaling (4.47) together in (4.37), we obtain

$$\begin{aligned} K_{\mathrm{Bulk}}(\hat{z}_1, \hat{z}_2) &= \lim_{h\to\infty} 4hK_{\mathrm{Edge}}(Z_1, Z_2) \\ &= \frac{2}{s\pi^{\frac{3}{2}}\Gamma(a+1)\kappa^{a+1}} \\ &\quad \times \left(\kappa - \frac{4\hat{y}_1^2}{s^2}\right)^{\frac{a}{2}} \left(\kappa - \frac{4\hat{y}_2^2}{s^2}\right)^{\frac{a}{2}} \int_0^1 \mathrm{d}c \frac{(cs/2)^{a+\frac{1}{2}}}{I_{a+\frac{1}{2}}(cs)} \cos\left(\frac{c}{\sqrt{\kappa}}(\hat{z}_1 - \bar{\hat{z}}_2)\right), \end{aligned} \tag{4.52}$$

which is similar to the asymptotic kernel (4.18) computed at the origin, in agreement with our conjecture.

5. Global correlations for unit weight $w(z) = 1$

In this section we will look at global correlation functions in the interior region (global regime) of the ellipse. Note that most of the N particles are concentrated in the vicinity of the edge of the ellipse due to the repulsion among them, and that only a negligibly small portion of the particles exist in the interior. In the simplest case of an unweighted ellipse, that is with weight $w(z) = 1$ corresponding to $a = 0$, we are able to derive the global asymptotic formulas for the correlation functions in the limit $N \to \infty$, which are valid in the whole interior of the ellipse.

Assuming $E \subset \mathbb{C}$ is a simply connected domain, t is a fixed point in E, and F is the conformal mapping (the Riemann map) of E onto the unit disc D, normalised by the conditions $F(t) = 0$ and $F'(t) > 0$. As is well-known, these conditions determine F uniquely.

Then, the following theorem [35, p 33] establishes the relationship between the Bergman kernel (called K_{global} below) and the Riemann map

Theorem (Unweighted case). *The conformal mapping F and the Bergman kernel function K_{global} of E are related as follows:*

$$K_{\text{global}}(z, \bar{t}) = \frac{1}{\pi} F'(z) F'(t) \quad \text{and} \quad F'(z) = \sqrt{\frac{\pi}{K_{\text{global}}(t, \bar{t})}} K_{\text{global}}(z, \bar{t}) \quad \text{for} \quad z \in E. \tag{5.1}$$

In particular when F is the Riemann mapping of the ellipse into unit disk, this is cumbersome, a first attempt for the Chebyshev polynomials of the second kind was made in [36]. However, our representation below will be somewhat more explicit, allowing for a consistency check in the rotationally symmetric limit, but we do not expect further simplification.

When setting $a = 0$ the Gegenbauer polynomials reduce to the Chebyshev polynomials of the second kind, $U_n(x) = C_n^{(1)}(x)$. Prior to taking the large-N limit we introduce the rescalings $z_j \mapsto z_j/\sqrt{2\tau}$ $(j = 1, 2)$, thus mapping the ellipse (2.2) to

$$E_{\text{rescaled}} = \left\{ z = x + \mathrm{i}y \,\middle|\, \frac{x^2}{1+\tau} + \frac{y^2}{1-\tau} \leqslant 1 \right\}, \quad 0 < \tau < 1\,. \tag{5.2}$$

This is done in order to be able to take the limit of maximal Hermiticity $\tau \to 0$ at the end of the calculation as a consistency check.

Setting $a = 0$ and rescaling the arguments, the kernel function (3.11) takes the form

$$K_N\left(\frac{z_1}{\sqrt{2\tau}}, \frac{z_2}{\sqrt{2\tau}}\right) = \frac{2\tau}{\pi\sqrt{1-\tau^2}} \sum_{n=0}^{N-1} \frac{n+1}{U_n(1/\tau)} U_n\left(\frac{z_1}{\sqrt{2\tau}}\right) U_n\left(\frac{\bar{z}_2}{\sqrt{2\tau}}\right). \tag{5.3}$$

We introduce a complex variable ω and a real variable v as

$$\frac{z}{\sqrt{2\tau}} = \frac{1}{2}\left(\omega + \frac{1}{\omega}\right), \quad \frac{1}{\tau} = \frac{1}{2}\left(v^2 + \frac{1}{v^2}\right), \tag{5.4}$$

which are uniquely determined for $z/\sqrt{2\tau} \notin (-1, 1)$ by satisfying the relations

$$1 \leqslant |\omega| < v\,. \tag{5.5}$$

This implies that z is in the interior of the ellipse (5.2). The parametrisation (5.4), also called Joukowsky map, allows to simplify the Chebyshev polynomials U_n, and we have [30]

$$U_n\left(\frac{z}{\sqrt{2\tau}}\right) = \frac{\omega^{n+1} - \omega^{-n-1}}{\omega - \omega^{-1}}, \quad U_n\left(\frac{1}{\tau}\right) = \frac{v^{2n+2} - v^{-2n-2}}{v^2 - v^{-2}}. \tag{5.6}$$

Putting these relations into the kernel, we obtain

$$K_N\left(\frac{z_1}{\sqrt{2\tau}},\frac{z_2}{\sqrt{2\tau}}\right)=\frac{4}{\pi}\frac{1}{(\omega_1-\omega_1^{-1})(\bar{\omega}_2-\bar{\omega}_2^{-1})}\times\sum_{n=0}^{N-1}(n+1)\frac{(\omega_1^{n+1}-\omega_1^{-n-1})(\bar{\omega}_2^{n+1}-\bar{\omega}_2^{-n-1})}{v^{2n+2}-v^{-2n-2}},\quad(5.7)$$

where

$$\frac{z_1}{\sqrt{2\tau}}=\frac{1}{2}\left(\omega_1+\frac{1}{\omega_1}\right),\quad\frac{z_2}{\sqrt{2\tau}}=\frac{1}{2}\left(\omega_2+\frac{1}{\omega_2}\right),\quad(5.8)$$

with $1\leqslant|\omega_1|<v$ and $1\leqslant|\omega_2|<v$. The sum can be rewritten as

$$K_N\left(\frac{z_1}{\sqrt{2\tau}},\frac{z_2}{\sqrt{2\tau}}\right)=\frac{4}{\pi}\frac{1}{(\omega_1-\omega_1^{-1})(\bar{\omega}_2-\bar{\omega}_2^{-1})}\times\sum_{j=0}^{\infty}\left.\frac{\partial}{\partial\lambda}\right|_{\lambda=1}\sum_{n=0}^{N-1}\left((\xi_j\omega_1\bar{\omega}_2)^{n+1}-(\xi_j\omega_1/\bar{\omega}_2)^{n+1}-(\xi_j\bar{\omega}_2/\omega_1)^{n+1}+(\xi_j/(\omega_1\bar{\omega}_2))^{n+1}\right),\quad(5.9)$$

by introducing the auxiliary variable

$$\xi_j=\frac{\lambda}{v^{2(1+2j)}}.\quad(5.10)$$

The differential operator

$$\left.\frac{\partial}{\partial\lambda}\right|_{\lambda=1}\quad(5.11)$$

means putting $\lambda=1$, after taking a derivative with respect to λ. We can now evaluate the sums over n as finite geometric series, and find

$$\begin{aligned}K_N\left(\frac{z_1}{\sqrt{2\tau}},\frac{z_2}{\sqrt{2\tau}}\right)=&\frac{4}{\pi}\frac{1}{(\omega_1-\omega_1^{-1})(\bar{\omega}_2-\bar{\omega}_2^{-1})}\\&\times\sum_{j=0}^{\infty}\left.\frac{\partial}{\partial\lambda}\right|_{\lambda=1}\left[(\xi_j\omega_1\bar{\omega}_2)\frac{1-(\xi_j\omega_1\bar{\omega}_2)^N}{1-(\xi_j\omega_1\bar{\omega}_2)}-(\xi_j\omega_1/\bar{\omega}_2)\frac{1-(\xi_j\omega_1/\bar{\omega}_2)^N}{1-(\xi_j\omega_1/\bar{\omega}_2)}\right.\\&\left.-(\xi_j\bar{\omega}_2/\omega_1)\frac{1-(\xi_j\bar{\omega}_2/\omega_1)^N}{1-(\xi_j\bar{\omega}_2/\omega_1)}+(\xi_j/(\omega_1\bar{\omega}_2))\frac{1-(\xi_j/(\omega_1\bar{\omega}_2))^N}{1-(\xi_j/(\omega_1\bar{\omega}_2))}\right].\end{aligned}\quad(5.12)$$

Because of $1\leqslant|\omega_1|<v$ and $1\leqslant|\omega_2|<v$, we observe that for all j

$$\left|\omega_1^{\pm1}\bar{\omega}_2^{\pm1}/v^{2(1+2j)}\right|<1\ .\quad(5.13)$$

Thus we can take the limit $N\to\infty$ (with τ fixed) to obtain

$$\begin{aligned}K_{\text{global}}(z_1,z_2)=&\lim_{N\to\infty}\frac{1}{2\tau}K_N\left(\frac{z_1}{\sqrt{2\tau}},\frac{z_2}{\sqrt{2\tau}}\right)\\=&\frac{2}{\pi\tau}\frac{1}{(\omega_1-\omega_1^{-1})(\bar{\omega}_2-\bar{\omega}_2^{-1})}\sum_{j=0}^{\infty}\left.\frac{\partial}{\partial\lambda}\right|_{\lambda=1}\left[\frac{\xi_j\omega_1\bar{\omega}_2}{1-(\xi_j\omega_1\bar{\omega}_2)}\right.\\&\left.-\frac{\xi_j\omega_1/\bar{\omega}_2}{1-(\xi_j\omega_1/\bar{\omega}_2)}-\frac{\xi_j\bar{\omega}_2/\omega_1}{1-(\xi_j\bar{\omega}_2/\omega_1)}+\frac{\xi_j/(\omega_1\bar{\omega}_2)}{1-(\xi_j/(\omega_1\bar{\omega}_2))}\right].\end{aligned}\quad(5.14)$$

Taking the derivative with respect to λ yields

$$K_{\text{global}}(z_1, z_2) = \frac{2}{\pi\tau} \frac{1}{(\omega_1 - \omega_1^{-1})(\bar{\omega}_2 - \bar{\omega}_2^{-1})} \times \sum_{j=0}^{\infty} \left[\frac{\eta_j \omega_1 \bar{\omega}_2}{(1 - (\eta_j \omega_1 \bar{\omega}_2))^2} - \frac{\eta_j \omega_1 / \bar{\omega}_2}{(1 - (\eta_j \omega_1 / \bar{\omega}_2))^2} - \frac{\eta_j \bar{\omega}_2 / \omega_1}{(1 - (\eta_j \bar{\omega}_2 / \omega_1))^2} + \frac{\eta_j / (\omega_1 \bar{\omega}_2)}{(1 - (\eta_j / (\omega_1 \bar{\omega}_2)))^2} \right], \tag{5.15}$$

with

$$\eta_j = \frac{1}{v^{2(1+2j)}}. \tag{5.16}$$

This is the limiting kernel on a global scale, valid in the entire interior of the ellipse (5.2). Because of (3.3) that remains valid in this limit, it determines all k-point correlation functions on a global scale. At present we are only able to derive such a global asymptotic formula for the simplest case $a = 0$. In appendices B and C we present a similar analysis for the Chebyshev polynomials of the first and third kind, with a non-flat measure on the ellipse.

To get an impression of the τ-dependence of the kernel, we consider the origin $z = 0$. Here, we can use $\omega = \pm i$ from (5.4), to obtain

$$K_{\text{global}}(0, 0) = \frac{2}{\pi\tau v^2} \sum_{j=0}^{\infty} v^{4j} \frac{v^{8j} + \frac{1}{v^4}}{\left(v^{8j} - \frac{1}{v^4}\right)^2}, \tag{5.17}$$

with the relation between v and τ from (5.4).

It is not justified to take the weak non-Hermiticity limit ($N \to \infty$ with the scaling (4.1)) of (5.15) because of the restriction (5.5) being violated, which was crucial for our analysis above. In the opposite limit of maximal non-Hermiticity $\tau \to 0$, which due to $1 < v$ and (5.4) implies that $v \to \infty$, we introduce the rescaled variables

$$\omega_j = v\zeta_j, \quad j = 1, 2, \tag{5.18}$$

with ζ_j fixed. Then, it follows that $z_j \sim \zeta_j$ in the limit $v \to \infty$. Moreover, in the sum of (5.15) only the first term $\eta_j \omega_1 \bar{\omega}_2 / (1 - (\eta_j \omega_1 \bar{\omega}_2))^2$ with $j = 0$ survives in the limit $v \to \infty$. We accordingly obtain for the global limiting kernel in the rotationally symmetric case

$$\lim_{\tau \to 0} K_{\text{global}}(z_1, z_2) = \frac{1}{\pi} \frac{1}{(1 - z_1 \bar{z}_2)^2}, \tag{5.19}$$

when $|z_j| < 1$ ($j = 1, 2$) according to (5.2). It is in agreement with the known result for the radially symmetric weight (2.8) with $a = 0$, as can be easily seen from the limit (4.30) of the corresponding kernel in (3.14).

6. Summary

In this paper (including appendices) we have introduced three new families (two were studied in appendix A) of Coulomb gases in two dimensions at the specific temperature $\beta = 2$, that are constrained to a hard-walled ellipse whose boundary is charged as well, and which repels a finite number of particles inside. In some examples in Appendices B and C the potentials include singularities at the foci of the ellipse. These results were made possible using the technique of planar orthogonal polynomials on that domain, together with newly derived orthogonality results for the classical polynomials of Gegenbauer and Jacobi type from a companion paper [23].

We have discussed the local correlation functions in large-N limit, at weak and strong non-Hermiticity in the bulk and at the edge of the spectrum, by determining the corresponding limiting kernels. We found several new universality classes of deformed sine- and Bessel-kernels in the complex plane, that all showed the influence of the edges. Several different families led to the same limiting kernel, thus underlying their conjectured universality. In the Hermitian limit we could recover the universal sine- and Bessel-kernel of the Jacobi ensemble. At strong non-Hermiticity we were led back to the corresponding limiting kernel of the ensemble of Gaussian and truncated unitary random matrices.

For the global correlation functions in the interior of the ellipse, we could only present partial results, based on the Chebyshev polynomials of the first, second and third kind.

It would be very interesting to find the global asymptotic formulas for all families of Coulomb gases presented here, perhaps taking a closer look at the Riemann mapping theorem. A further direction of investigation is a comparison with the local correlations of both the standard elliptic Ginibre ensemble, and that with a hard constraint imposed. A popular tool in comparison with data is the number variance. Although it follows from the kernel it remains to be seen, if it could be further simplified in the various limits we have taken.

Acknowledgments

The work of TN was partially supported by the Japan Society for the Promotion of Science (KAKENHI 25400397). GA & MK acknowledge support by the German research council through CRC1283: 'Taming uncertainty and profiting from randomness and low regularity in analysis, stochastics and their applications'. GA also thanks the Niels Bohr International Academy for hospitality where part of this work was done. IP thanks support by the grant DAAD-CONICYT/Becas Chile, 2016/91609937. We thank Yacin Ameur for insightful discussions about the hard edge scaling limit.

Appendix A. Two families of asymmetric Jacobi polynomials

In this appendix we study the weak non-Hermiticity limit for two further families of planar orthogonal polynomials derived in [23]. Let us give a reason for the existence of these classes in addition to (3.5). As we saw in the transformations (4.11) and (4.14) of the Gegenbauer polynomials—which are usually expressed in terms of the Jacobi polynomials with symmetric indices (3.17)—these can also be mapped to the Jacobi polynomials $P_n^{\left(a+\frac{1}{2},\pm\frac{1}{2}\right)}(z)$. By using these mappings, one can see that the resulting Jacobi polynomials are also orthogonal on the same ellipse, but with different weights. In this appendix, we evaluate the asymptotic behaviour of the Coulomb gas associated to those weights.

A.1. The Jacobi polynomials $P_n^{\left(a+\frac{1}{2},\frac{1}{2}\right)}(z)$

It is shown in [23] that the Jacobi polynomials $P_n^{\left(a+\frac{1}{2},\frac{1}{2}\right)}(z)$ satisfy the orthogonality relation

$$\begin{aligned}&\int_E \mathrm{d}^2 z\, w_+(z) P_m^{\left(a+\frac{1}{2},\frac{1}{2}\right)}(z) P_n^{\left(a+\frac{1}{2},\frac{1}{2}\right)}(\bar{z})\\ &= 4\sqrt{\frac{1-\tau}{2\tau}}\,\frac{\Gamma(n+\frac{3}{2})^2\Gamma(a+1)^2}{(2n+a+2)\Gamma(n+a+2)^2}\,C_{2n+1}^{(a+1)}\left(\sqrt{\frac{1+\tau}{2\tau}}\right)\delta_{mn},\end{aligned} \tag{A.1}$$

where $a > -1$, E is the elliptic domain (2.2), and $C_n^{(a+1)}(z)$ are the Gegenbauer polynomials (3.6). The one-particle weight function $w(z)$ in (2.4) defining this type of Coulomb gas takes the form

$$w_+(z) = (1 - \mu(z))^a, \tag{A.2}$$

and

$$\mu(z) = \frac{2\tau}{1-\tau}\left(\sqrt{\frac{1+\tau}{2\tau}}\sqrt{(1+x)^2+y^2} - 1 - x\right), \tag{A.3}$$

with $z = x + \mathrm{i}y$. This weight function is different from (2.5), except in the case $a = 0$, when the indices of the Jacobi polynomials again become symmetric. Note that the monic orthogonal polynomials $M_n(z) = z^n + \cdots$ are given by [31]

$$M_n(z) = 2^n n! \frac{\Gamma(n+a+2)}{\Gamma(2n+a+2)} P_n^{\left(a+\frac{1}{2},\frac{1}{2}\right)}(z). \tag{A.4}$$

We obtain the kernel $K_N(z_1, z_2)$ in (3.4) as

$$\begin{aligned} K_N(z_1,z_2) = {} & \frac{1}{4}(1-\mu(z_1))^{a/2}(1-\mu(\bar{z}_2))^{a/2}\sqrt{\frac{2\tau}{1-\tau}}\frac{1}{\Gamma(a+1)^2} \\ & \times \sum_{n=0}^{N-1} \frac{(2n+a+2)\Gamma(n+a+2)^2}{\Gamma(n+\frac{3}{2})^2 C_{2n+1}^{(a+1)}\left(\sqrt{(1+\tau)/(2\tau)}\right)} P_n^{\left(a+\frac{1}{2},\frac{1}{2}\right)}(z_1) P_n^{\left(a+\frac{1}{2},\frac{1}{2}\right)}(\bar{z}_2). \end{aligned} \tag{A.5}$$

In the following, we will evaluate the asymptotic forms of this kernel in the weak non-Hermiticity limit at the edges, that is around the foci of the ellipse $z = +1$ and $z = -1$. Because in section 4 we have seen that the bulk limit can be recovered from the edge limit, we will first derive the latter. However, due to the indices of the Jacobi polynomials now being non-symmetric, we expect the limits at the endpoints ± 1 to be different, because of the lack of parity symmetry, see (4.4).

(1) *Edge limit at the focus $z = +1$:*
In order to magnify this region, we recall the weak non-Hermiticity limit (4.1)

$$\frac{1}{\tau} = 1 + \frac{s^2}{2N^2}, \tag{A.6}$$

and the rescaling (4.32) around the right focus $+1$:

$$z_j = 1 - \frac{Z_j}{2N^2}, \quad j = 1, 2. \tag{A.7}$$

We will take the double scaling limit $N \to \infty$ and $\tau \to 1$ such that the positive number s and complex numbers $Z_j = X_j + \mathrm{i}Y_j$ are kept fixed. In this scaling limit the function inside the weight (A.2) gets mapped to

$$1 - \mu\left(1 - \frac{Z}{2N^2}\right) \sim \frac{1}{4N^2}\left(\frac{s^2}{4} + X - \frac{Y^2}{s^2}\right), \tag{A.8}$$

from which we can read off the domain of our scaling variables, being in the parabolic domain (4.34). Here $Z = X + \mathrm{i}Y$ is kept fixed. In analogy to (4.17) we have

$$C_{2n+1}^{(a+1)}\left(\sqrt{\frac{1+\tau}{2\tau}}\right) \sim N^{2a+1}\frac{\Gamma(a+\frac{3}{2})}{\Gamma(2a+2)}\left(\frac{s}{8c}\right)^{-a-\frac{1}{2}} I_{a+\frac{1}{2}}(cs), \tag{A.9}$$

with the ratio $c = n/N$ being kept fixed. Using (4.3), we can readily find the asymptotic for the polynomials

$$P_n^{(a+\frac{1}{2},\frac{1}{2})}\left(1-\frac{Z}{2N^2}\right) \sim N^{a+\frac{1}{2}}\left(\frac{\sqrt{Z}}{2}\right)^{-a-\frac{1}{2}} J_{a+\frac{1}{2}}\left(c\sqrt{Z}\right). \tag{A.10}$$

Putting these asymptotic formulas together with the identities (4.2) into (A.5), and replacing the sum by an integral, we obtain exactly the same asymptotic formula (4.37) for $K_{\mathrm{Edge}}(Z_1,Z_2) = \lim_{N\to\infty} K_N(z_1,z_2)/(4N^4)$. This fact indicates the universality of this kernel.

The Hermitian and strongly non-Hermitian limit as well as the bulk limit then follow as in section 4.2.

(2) *Edge limit at the focus $z = -1$:*

Next, we use the scaling in the weak non-Hermiticity limit (A.6) and magnify the region around the left focus $z = -1$ in the same way as in (A.7):

$$z_j = -1 + \frac{Z_j}{2N^2}, \quad j = 1, 2, \tag{A.11}$$

with $s > 0$ and $Z_j = X_j + \mathrm{i}Y_j$ fixed in the limit $N \to \infty$. It is straightforward to derive the asymptotic form of the weight function

$$1 - \mu\left(-1 + \frac{Z}{2N^2}\right) \sim 1 - \frac{2}{s^2}\left(\sqrt{X^2+Y^2} - X\right). \tag{A.12}$$

Here $Z = X + \mathrm{i}Y$ is kept fixed. For this factor to be non-negative it can be seen that the points (X_j, Y_j) have to lie inside the parabolic domain (4.34). For the asymptotic form of the Jacobi polynomials with non-symmetric indices we have

$$P_n^{(a+\frac{1}{2},\frac{1}{2})}\left(-1+\frac{Z}{2N^2}\right) = (-1)^n P_n^{(\frac{1}{2},a+\frac{1}{2})}\left(1-\frac{Z}{2N^2}\right) \sim (-1)^n N^{\frac{1}{2}}\left(\frac{\sqrt{Z}}{2}\right)^{-\frac{1}{2}} J_{\frac{1}{2}}\left(c\sqrt{Z}\right), \tag{A.13}$$

in the limit $N \to \infty$, after using (4.4) and (4.3). These asymptotic formulas together with (A.9) are put into the kernel (A.5) and yield

$$\begin{aligned} K_{\mathrm{Edge}}(Z_1,Z_2) &= \lim_{N\to\infty}\frac{1}{4N^4}K_N(z_1,z_2) \\ &= \frac{(s/2)^{a-\frac{1}{2}}}{4\sqrt{\pi}\Gamma(a+1)}\left(1-\frac{2}{s^2}(|Z_1|-X_1)\right)^{a/2}\left(1-\frac{2}{s^2}(|Z_2|-X_2)\right)^{a/2} \\ &\quad\times\left(\sqrt{Z_1\bar{Z}_2}\right)^{-\frac{1}{2}}\int_0^1 \mathrm{d}c\, \frac{c^{a+\frac{3}{2}}}{I_{a+\frac{1}{2}}(cs)} J_{\frac{1}{2}}\left(c\sqrt{Z_1}\right) J_{\frac{1}{2}}\left(c\sqrt{\bar{Z}_2}\right). \\ &= \frac{(s/2)^{a-\frac{1}{2}}}{2\pi^{3/2}\Gamma(a+1)}\left(1-\frac{2}{s^2}(|Z_1|-X_1)\right)^{a/2}\left(1-\frac{2}{s^2}(|Z_2|-X_2)\right)^{a/2} \\ &\quad\times\frac{1}{\sqrt{Z_1\bar{Z}_2}}\int_0^1 \mathrm{d}c\, \frac{c^{a+\frac{1}{2}}}{I_{a+\frac{1}{2}}(cs)} \sin\left(c\sqrt{Z_1}\right)\sin\left(c\sqrt{\bar{Z}_2}\right). \end{aligned} \tag{A.14}$$

In the last step the J-Bessel functions are expressed in terms of sine, using (4.16). For $a \neq 0$ this edge kernel is clearly different from the one obtained for the Gegenbauer polynomials in (4.37) in section 4.2. While the local asymptotic form of the Jacobi polynomials around this focal point yields $J_{\frac{1}{2}}$ (represented by means of the sine function), the influence of the edge is obviously still present through the dependence of the other factors on a.

In the Hermitian limit $s \to 0$, the coordinates (X_j, Y_j) are confined to the domain satisfying $X_j \geqslant 0$ and $Y_j = 0$, as we saw already in the section 4.2. Using (4.20) and normalising the area as in (4.39), we find the asymptotic formula

$$\begin{aligned}
&\lim_{s\to 0} \frac{s\pi}{2(a+1)B} K_{\mathrm{Edge}}(Z_1, Z_2)\bigg|_{X_{1,2}\geqslant 0, Y_{1,2}=0} \\
&= \frac{1}{4}\left(X_1X_2\right)^{-\frac{1}{4}} \int_0^1 \mathrm{d}c\, c\, J_{\frac{1}{2}}\left(c\sqrt{X_1}\right) J_{\frac{1}{2}}\left(c\sqrt{X_2}\right). \qquad \text{(A.15)}
\end{aligned}$$

It agrees with the Bessel-kernel of the Jacobi ensemble (4.39) at $a = 0$.

In the strong non-Hermiticity limit $s \to \infty$ we use the scaling variables $\tilde{X}_j$ and $\tilde{Y}_j$ defined in (4.40), together with the asymptotic relation

$$1 - \frac{2}{s^2}\left(|Z_j| - X_j\right) \sim \frac{2}{s}\tilde{X}_j, \quad s \to \infty, \qquad \text{(A.16)}$$

and (4.41). The resulting limit $\lim_{s\to\infty}(s^2/4)K_{\mathrm{Edge}}(Z_1, Z_2)$ exactly reproduces the formula (4.44).

The bulk limit $h \to \infty$, with the scaling variables $\hat{z}_j = \hat{x}_j + \mathrm{i}\hat{y}_j$ defined as in (4.47) by $Z_j = \kappa h - 2\sqrt{h}\hat{z}_j$ $(\kappa > 0)$, can be evaluated by means of the relation

$$1 - \frac{2}{s^2}\left(|Z_j| - X_j\right) \sim 1 - \frac{4}{\kappa s^2}\hat{y}_j^2, \quad h \to \infty, \qquad \text{(A.17)}$$

and (4.41). As a result we obtain exactly the same formula (4.52) for the asymptotic kernel $K_{\mathrm{Bulk}}(\hat{z}_1, \hat{z}_2) = \lim_{h\to\infty} 4hK_{\mathrm{Edge}}(Z_1, Z_2)$. From this, we again conjecture that the bulk scaling limit has a similar form, when we zoom into any point $x_0 \in (-1, 1)$. Thus all three limits of the kernel (A.14) lead back to the classes we have already found in section 4.

A.2. The Jacobi polynomials $P_n^{(a+\frac{1}{2},-\frac{1}{2})}(z)$

The Jacobi polynomials $P_n^{(a+\frac{1}{2},-\frac{1}{2})}(z)$ satisfy the orthogonality relation [23]

$$\begin{aligned}
&\int_E \mathrm{d}^2 z\, w_-(z) P_m^{(a+\frac{1}{2},-\frac{1}{2})}(z) P_n^{(a+\frac{1}{2},-\frac{1}{2})}(\bar{z}) \\
&= 2\sqrt{\frac{1-\tau}{2\tau}} \frac{\Gamma(n+\frac{1}{2})^2\Gamma(a+1)^2}{(2n+a+1)\Gamma(n+a+1)^2} C_{2n}^{(a+1)}\left(\sqrt{\frac{1+\tau}{2\tau}}\right)\delta_{mn}, \qquad \text{(A.18)}
\end{aligned}$$

where $a > -1$, E is the elliptic domain (2.2), and $C_n^{(a+1)}(z)$ are the Gegenbauer polynomials (3.6). Moreover, $w(z)$ in (2.4) takes the form

$$w_-(z) = \frac{(1-\mu(z))^a}{|1+z|}, \tag{A.19}$$

with $\mu(z)$ defined in (A.3). Notice that also for $a = 0$ the polynomials and weight are different from those in section 3.

The monic orthogonal polynomials $M_n(z) = z^n + \cdots$ are given by [31]

$$M_n(z) = 2^n n! \frac{\Gamma(n+a+1)}{\Gamma(2n+a+1)} P_n^{\left(a+\frac{1}{2},-\frac{1}{2}\right)}(z), \tag{A.20}$$

and for the kernel function $K_N(z_1,z_2)$ in (3.4) we obtain from the above

$$\begin{aligned} K_N(z_1,z_2) = &\frac{(1-\mu(z_1))^{a/2}(1-\mu(\bar{z}_2))^{a/2}}{2|1+z_1|^{1/2}|1+z_2|^{1/2}} \sqrt{\frac{2\tau}{1-\tau}} \frac{1}{\Gamma(a+1)^2} \\ &\times \sum_{n=0}^{N-1} \frac{(2n+a+1)\Gamma(n+a+1)^2}{\Gamma(n+\frac{1}{2})^2\, C_{2n}^{(a+1)}\left(\sqrt{(1+\tau)/(2\tau)}\right)} P_n^{\left(a+\frac{1}{2},-\frac{1}{2}\right)}(z_1) P_n^{\left(a+\frac{1}{2},-\frac{1}{2}\right)}(\bar{z}_2). \end{aligned} \tag{A.21}$$

As in the previous subsection we will first determine the weak non-Hermiticity limit at the edges.

(1) *Edge limit at the focus $z = +1$*
In the vicinity of the focus $+1$, we can again utilise the scalings (A.6) and (A.7), finding the same domain (4.34) as before. From (4.3), we find

$$P_n^{\left(a+\frac{1}{2},-\frac{1}{2}\right)}\left(1-\frac{Z}{2N^2}\right) \sim N^{a+\frac{1}{2}} \left(\frac{\sqrt{Z}}{2}\right)^{-a-\frac{1}{2}} J_{a+\frac{1}{2}}\left(c\sqrt{Z}\right), \tag{A.22}$$

in the limit $N \to \infty$. It agrees with (A.13) because of its independence of the second index of the Jacobi polynomials.
We put this together with (A.9)—which does not change to leading order under the shift $2n+1 \mapsto 2n$—and (A.8) into (A.21), and again find exactly the same asymptotic formula (4.37) for $K_{\mathrm{Edge}}(Z_1,Z_2) = \lim_{N\to\infty} K_N(z_1,z_2)/(4N^4)$. After the analysis of the previous subsection this universality is not unexpected. The corresponding limits to Hermiticity, strong non-Hermiticity and the bulk thus follow alike.

(2) *Edge limit at the focus $z = -1$*
Finally we use the scalings (A.6) and (A.11) to study the asymptotic behaviour of the kernel in the vicinity of $z = -1$. As in the previous subsection the coordinates (X_j, Y_j) are in the domain (4.34). For the asymptotic behaviour we now find

$$P_n^{\left(a+\frac{1}{2},-\frac{1}{2}\right)}\left(-1+\frac{Z}{2N^2}\right) \sim (-1)^n N^{-1/2} \left(\frac{\sqrt{Z}}{2}\right)^{1/2} J_{-1/2}\left(c\sqrt{Z}\right), \tag{A.23}$$

in the limit $N \to \infty$, due to (4.4) and (4.3). This formula (A.9) being also true for shifted index $2n+1 \mapsto 2n$, and (A.12) are put into the kernel (A.21). The result is

$$
\begin{aligned}
K_{\text{Edge}}(Z_1,Z_2) &= \lim_{N\to\infty}\frac{1}{4N^4}K_N(z_1,z_2)\\
&= \frac{(s/2)^{a-\frac{1}{2}}}{4\sqrt{\pi}\Gamma(a+1)}\left(1-\frac{2}{s^2}\left(|Z_1|-X_1\right)\right)^{a/2}\left(1-\frac{2}{s^2}\left(|Z_2|-X_2\right)\right)^{a/2}\\
&\quad\times\left(\frac{\sqrt{Z_1\bar{Z}_2}}{|Z_1Z_2|}\right)^{\frac{1}{2}}\int_0^1 \mathrm{d}c\,\frac{c^{a+\frac{3}{2}}}{I_{a+\frac{1}{2}}(cs)}J_{-\frac{1}{2}}\left(c\sqrt{Z_1}\right)J_{-\frac{1}{2}}\left(c\sqrt{\bar{Z}_2}\right)\\
&= \frac{(s/2)^{a-\frac{1}{2}}}{2\pi^{3/2}\Gamma(a+1)}\left(1-\frac{2}{s^2}\left(|Z_1|-X_1\right)\right)^{a/2}\left(1-\frac{2}{s^2}\left(|Z_2|-X_2\right)\right)^{a/2}\\
&\quad\times|Z_1Z_2|^{-1/2}\int_0^1 \mathrm{d}c\,\frac{c^{a+\frac{1}{2}}}{I_{a+\frac{1}{2}}(cs)}\cos\left(c\sqrt{Z_1}\right)\cos\left(c\sqrt{\bar{Z}_2}\right).
\end{aligned}
\tag{A.24}
$$

In the last step we used (4.13), expressing the J-Bessel functions through cosine. Once again this edge kernel is different from that in (4.37) in section 4.2, with the influence of the edge clearly visible through the dependence on a.
In the Hermitian limit $s\to 0$, we again put (X_j,Y_j) in the domain satisfying $X_j\geqslant 0$ and $Y_j=0$. As before (4.20) leads to

$$
\begin{aligned}
&\lim_{s\to 0}\frac{s\pi}{2(a+1)B}K_{\text{Edge}}(Z_1,Z_2)\bigg|_{X_{1,2}\geqslant 0,Y_{1,2}=0}\\
&=\frac{1}{4}\left(X_1X_2\right)^{-\frac{1}{4}}\int_0^1 \mathrm{d}c\,c\,J_{-\frac{1}{2}}\left(c\sqrt{X_1}\right)J_{-\frac{1}{2}}\left(c\sqrt{X_2}\right),
\end{aligned}
\tag{A.25}
$$

which agrees with (4.39) continued to $a=-1$,

In the strong non-Hermiticity limit $s\to\infty$ we use the scalings (4.40) and the asymptotic relations (A.16) and (4.41). It follows that $\lim_{s\to\infty}(s^2/4)K_{\text{Edge}}(Z_1,Z_2)$ is identical to the result in (4.44).

The bulk limit $h\to\infty$ with the scaling (4.47) can be treated along the same line as in the previous subsection, by using (A.17) and (4.41). We find exactly the same formula (4.52) for $K_{\text{Bulk}}(\hat{z}_1,\hat{z}_2)=\lim_{h\to\infty}4hK_{\text{Edge}}(Z_1,Z_2)$. We again conjecture that a similar bulk asymptotic form holds for this model. Also for these polynomials all three limits lead back to known results.

Appendix B. Correlations for Chebyshev polynomials of 1st kind

In this appendix we will derive the limiting microscopic and global kernel for the Chebyshev polynomials of the first kind $T_n(z)$. The orthogonality relation was previously known [30], see [23, corollary 4.4], but it does not follow directly from that of the Gegenbauer polynomials presented in section 3:

$$
\int_E d^2z\,w_I(z)T_m(z)T_n(\bar{z}) = \begin{cases}\dfrac{\pi}{2n}\sqrt{\dfrac{1-\tau}{2\tau}}\,C^{(1)}_{2n-1}\left(\sqrt{\dfrac{1+\tau}{2\tau}}\right)\delta_{mn}, & m>0, n\geqslant 0,\\ 2\pi\log v, & m=n=0,\end{cases}
\tag{B.1}
$$

on the ellipse (2.2), where

$$
w_I(z)=\frac{1}{|1-z^2|},
\tag{B.2}
$$

and

$$v = \frac{\sqrt{1+\tau}+\sqrt{1-\tau}}{\sqrt{2\tau}}, \quad 0 < \tau < 1\,. \tag{B.3}$$

The weight function $w(z)$ of the corresponding Coulomb gas model (2.4) is given by $w_I(z)$, with singularities at the foci ± 1. The Chebyshev polynomials of the first kind are

$$T_n(z) = \sqrt{\pi}\frac{\Gamma(n+1)}{\Gamma(n+\frac{1}{2})}P_n^{(-\frac{1}{2},-\frac{1}{2})}(z), \tag{B.4}$$

in terms of the Jacobi polynomials, which are again symmetric. Note that the corresponding monic orthogonal polynomials are $M_n(z) = 2^{-n+1}T_n(z)$ for $n \geqslant 1$, and $M_0(z) = T_0(z) = 1$. We find the kernel in (3.11) with $w(z) = w_I(z)$ as

$$\begin{aligned} K_N(z_1,z_2) &= \frac{1}{\pi}\frac{1}{\sqrt{|1-z_1^2||1-\bar{z}_2^2|}} \\ &\times \left[\sqrt{\frac{2\tau}{1-\tau}}\sum_{n=1}^{N-1}\frac{2n}{C_{2n-1}^{(1)}\left(\sqrt{(1+\tau)/(2\tau)}\right)}T_n(z_1)T_n(\bar{z}_2)+\frac{1}{2\log v}\right]. \end{aligned} \tag{B.5}$$

B.1. Local edge scaling limit

In order to evaluate the asymptotic behaviour of this kernel around the focus $z = 1$, we again adopt the scalings (A.6) and (A.7). Because the polynomials have parity we only need to analyse one of the foci. It can readily be seen from (4.3) that

$$T_n\left(1-\frac{Z}{2N^2}\right) \sim \sqrt{\pi}c^{1/2}\left(\frac{\sqrt{Z}}{2}\right)^{1/2}J_{-\frac{1}{2}}\left(c\sqrt{Z}\right), \tag{B.6}$$

in the limit $N \to \infty$ with $c = n/N$ fixed. We use this formula, (A.9) valid to leading order at shifted index $2n+1 \mapsto 2n-1$, and the expansion

$$v^2 \sim 1 + \frac{s}{N}, \quad N \to \infty, \tag{B.7}$$

that follows from (4.2). Inserting them into (B.5) we obtain

$$\begin{aligned} K_{\mathrm{Edge}}(Z_1,Z_2) &= \lim_{N\to\infty}\frac{1}{4N^4}K_N(z_1,z_2) \\ &= \frac{1}{4}\sqrt{\frac{2}{s\pi}}\left(\frac{\sqrt{Z_1\bar{Z}_2}}{|Z_1Z_2|}\right)^{\frac{1}{2}}\int_0^1 \mathrm{d}c\,\frac{c^{\frac{3}{2}}}{I_{\frac{1}{2}}(cs)}J_{-\frac{1}{2}}\left(c\sqrt{Z_1}\right)J_{-\frac{1}{2}}\left(c\sqrt{\bar{Z}_2}\right), \end{aligned} \tag{B.8}$$

which is identical to (A.24) with $a = 0$. Consequently, this kernel is also universal, and the corresponding Hermitian, strongly non-Hermitian and bulk limits follow as discussed in section A.2.

B.2. Global correlations

In order to derive a global asymptotic formula for the kernel, we use the relations [30]

$$T_n\left(\frac{z}{\sqrt{2\tau}}\right)=\frac{1}{2}\left(\omega^n+\frac{1}{\omega^n}\right),\quad \frac{z}{\sqrt{2\tau}}=\frac{1}{2}\left(\omega+\frac{1}{\omega}\right), \tag{B.9}$$

and

$$\sqrt{\frac{1-\tau}{2\tau}}C_{2n-1}^{(1)}\left(\sqrt{\frac{1+\tau}{2\tau}}\right)=\sqrt{\frac{1-\tau}{2\tau}}U_{2n-1}\left(\sqrt{\frac{1+\tau}{2\tau}}\right)=\frac{1}{2}\left(v^{2n}-\frac{1}{v^{2n}}\right) \tag{B.10}$$

(from (5.4) together with (5.6)), in (B.5) to find

$$\begin{aligned}K_N\left(\frac{z_1}{\sqrt{2\tau}},\frac{z_2}{\sqrt{2\tau}}\right)&=\frac{1}{\pi}\left|1-\frac{z_1^2}{2\tau}\right|^{-1/2}\left|1-\frac{\bar{z}_2^2}{2\tau}\right|^{-1/2}\\&\times\left[\sum_{n=1}^{N-1}\frac{n}{v^{2n}-v^{-2n}}\left(\omega_1^n+\frac{1}{\omega_1^n}\right)\left(\bar{\omega}_2^n+\frac{1}{\bar{\omega}_2^n}\right)+\frac{1}{2\log v}\right].\end{aligned} \tag{B.11}$$

Here, we define $z_1/\sqrt{2\tau}=(\omega_1+\omega_1^{-1})/2$ and $z_2/\sqrt{2\tau}=(\omega_2+\omega_2^{-1})/2$. As $z_1/\sqrt{2\tau}$ and $z_2/\sqrt{2\tau}$ are in the interior of the ellipse (2.2), the conditions $1\leqslant|\omega_1|<v$ and $1\leqslant|\omega_2|<v$ uniquely fix ω_1 and ω_2 for $z_1/\sqrt{2\tau},z_2/\sqrt{2\tau}\notin(-1,1)$. Now, in order to take the limit $N\to\infty$, up to a pre-factor, we can use the same argument as in section 5. The result is

$$\begin{aligned}K_{\rm global}(z_1,z_2)&=\lim_{N\to\infty}\frac{1}{2\tau}K_N\left(\frac{z_1}{\sqrt{2\tau}},\frac{z_2}{\sqrt{2\tau}}\right)\\&=\frac{1}{2\pi\tau}\left|1-\frac{z_1^2}{2\tau}\right|^{-1/2}\left|1-\frac{\bar{z}_2^2}{2\tau}\right|^{-1/2}\\&\times\left[\sum_{j=0}^{\infty}\left(\frac{\eta_j\omega_1\bar{\omega}_2}{(1-(\eta_j\omega_1\bar{\omega}_2))^2}+\frac{\eta_j\omega_1/\bar{\omega}_2}{(1-(\eta_j\omega_1/\bar{\omega}_2))^2}\right.\right.\\&\left.\left.+\frac{\eta_j\bar{\omega}_2/\omega_1}{(1-(\eta_j\bar{\omega}_2/\omega_1))^2}+\frac{\eta_j/(\omega_1\bar{\omega}_2)}{(1-(\eta_j/(\omega_1\bar{\omega}_2)))^2}\right)+\frac{1}{2\log v}\right],\end{aligned} \tag{B.12}$$

with $\eta_j=1/v^{2(1+2j)}$.

Moreover, we can take the radially symmetric limit $\tau\to0$ ($v\to\infty$) and introducing the same scaling arguments as in (5.18) to obtain

$$\lim_{\tau\to0}K_{\rm global}(z_1,z_2)=\frac{1}{\pi|z_1||z_2|}\frac{z_1\bar{z}_2}{(1-z_1\bar{z}_2)^2}, \tag{B.13}$$

when $0<|z_j|<1$, $j=1,2$. In the domain of validity this kernel is equivalent to the one in (5.19).

Appendix C. Correlations for Chebyshev polynomials of 3rd kind

A similar procedure to that in appendix B can be applied to the Coulomb gas model (2.4), with the weight function $w(z)$ given by

$$w_{III}(z)=\frac{1}{|1+z|}\quad\text{or}\quad w_{IV}(z)=\frac{1}{|1-z|}. \tag{C.1}$$

These models correspond to the Chebyshev polynomials of the third and fourth kind, respectively. It should be noted that the model with $w_{III}(z)$ is a special case $a=0$ of the model studied in section A.2. Moreover the model with $w_{IV}(z)$ is an image under the mapping $z \to -z$ of the model with $w_{III}(z)$. Therefore, in the following, we only treat the global asymptotic formulas for the model with $w_{III}(z)$. The corresponding Chebyshev polynomials of the third kind

$$V_n(z) = \frac{2n+1}{P_n^{\left(\frac{1}{2},-\frac{1}{2}\right)}(1)} P_n^{\left(\frac{1}{2},-\frac{1}{2}\right)}(z), \tag{C.2}$$

satisfy the orthogonality relation [30]

$$\int_E \mathrm{d}^2 z\, w_{III}(z) V_m(z) V_n(\bar{z}) = \frac{2\pi}{2n+1} \sqrt{\frac{1-\tau}{2\tau}} C_{2n}^{(1)} \left(\sqrt{\frac{1+\tau}{2\tau}} \right) \delta_{mn}, \tag{C.3}$$

with $m, n = 0, 1, 2, \cdots$. The corresponding monic orthogonal polynomials are $M_n(z) = 2^{-n} V_n(z)$. We use the relations [30]

$$V_n\left(\frac{z}{\sqrt{2\tau}}\right) = \frac{\omega^{n+\frac{1}{2}} + \omega^{-n-\frac{1}{2}}}{w^{\frac{1}{2}} + w^{-\frac{1}{2}}}, \quad \frac{z}{\sqrt{2\tau}} = \frac{1}{2}\left(\omega + \frac{1}{\omega}\right), \tag{C.4}$$

and

$$\sqrt{\frac{1-\tau}{2\tau}} C_{2n}^{(1)} \left(\sqrt{\frac{1+\tau}{2\tau}} \right) = \sqrt{\frac{1-\tau}{2\tau}} U_{2n} \left(\sqrt{\frac{1+\tau}{2\tau}} \right) = \frac{1}{2}\left(v^{2n+1} - \frac{1}{v^{2n+1}} \right), \tag{C.5}$$

to obtain the kernel function in (3.4) with $w(z) = w_{III}(z)$. Here, v is defined in (B.3). The result is

$$\begin{aligned} K_N\left(\frac{z_1}{\sqrt{2\tau}}, \frac{z_2}{\sqrt{2\tau}}\right) &= \frac{1}{\pi} \left| 1 + \frac{z_1}{\sqrt{2\tau}} \right|^{-1/2} \left| 1 + \frac{\bar{z}_2}{\sqrt{2\tau}} \right|^{-1/2} \\ &\times \sum_{n=0}^{N-1} \frac{2n+1}{v^{2n+1} - v^{-2n-1}} \frac{\left(\omega_1^{n+\frac{1}{2}} + \omega_1^{-n-\frac{1}{2}}\right)\left(\bar{\omega}_2^{n+\frac{1}{2}} + \bar{\omega}_2^{-n-\frac{1}{2}}\right)}{\left(\omega_1^{\frac{1}{2}} + \omega_1^{-\frac{1}{2}}\right)\left(\bar{\omega}_2^{\frac{1}{2}} + \bar{\omega}_2^{-\frac{1}{2}}\right)}, \end{aligned} \tag{C.6}$$

where $z_1/\sqrt{2\tau} = (\omega_1 + (1/\omega_1))/2$ and $z_2/\sqrt{2\tau} = (\omega_2 + (1/\omega_2))/2$, and again $1 \leqslant |\omega_1| < v$ and $1 \leqslant |\omega_2| < v$. As before we use an argument similar to that employed in section 5 and appendix B, and find

$$\begin{aligned} K_{\mathrm{global}}(z_1, z_2) &= \lim_{N\to\infty} \frac{1}{2\tau} K_N\left(\frac{z_1}{\sqrt{2\tau}}, \frac{z_2}{\sqrt{2\tau}}\right) \\ &= \frac{1}{2\pi\tau} \left| 1 + \frac{z_1}{\sqrt{2\tau}} \right|^{-1/2} \left| 1 + \frac{\bar{z}_2}{\sqrt{2\tau}} \right|^{-1/2} \frac{1}{\left(\omega_1^{\frac{1}{2}} + \omega_1^{-\frac{1}{2}}\right)\left(\bar{\omega}_2^{\frac{1}{2}} + \bar{\omega}_2^{-\frac{1}{2}}\right)} \\ &\times \sum_{j=0}^{\infty} \left[\frac{(\eta_j \omega_1 \bar{\omega}_2)^{1/2}(1 + (\eta_j \omega_1 \bar{\omega}_2))}{(1 - (\eta_j \omega_1 \bar{\omega}_2))^2} + \frac{(\eta_j \omega_1/\bar{\omega}_2)^{1/2}(1 + (\eta_j \omega_1/\bar{\omega}_2))}{(1 - (\eta_j \omega_1/\bar{\omega}_2))^2} \right. \\ &\left. + \frac{(\eta_j \bar{\omega}_2/\omega_1)^{1/2}(1 + (\eta_j \bar{\omega}_2/\omega_1))}{(1 - (\eta_j \bar{\omega}_2/\omega_1))^2} + \frac{(\eta_j/(\omega_1 \bar{\omega}_2))^{1/2}(1 + (\eta_j/(\omega_1 \bar{\omega}_2)))}{(1 - (\eta_j/(\omega_1 \bar{\omega}_2)))^2} \right], \end{aligned} \tag{C.7}$$

with $\eta_j = 1/v^{2(1+2j)}$. We can moreover take the radially symmetric limit $\tau \to 0$ ($v \to \infty$) and obtain

$$\lim_{\tau \to 0} K_{\text{global}}(z_1, z_2) = \frac{1}{2\pi\sqrt{|z_1||z_2|}} \frac{1 + z_1\bar{z}_2}{(1 - z_1\bar{z}_2)^2}, \tag{C.8}$$

when $0 < |z_j| < 1$ $(j = 1, 2)$. It differs from (B.13) and (5.19).

ORCID iDs

Taro Nagao https://orcid.org/0000-0003-1028-7159
Gernot Akemann https://orcid.org/0000-0002-1710-4258
Mario Kieburg https://orcid.org/0000-0001-8864-6022

References

[1] Ginibre J 1965 Statistical ensembles of complex, quaternion, and real matrices *J. Math. Phys.* **6** 440–9
[2] Forrester P J 2016 Analogies between random matrix ensembles and the one-component plasma in two-dimensions *Nucl. Phys.* B **904** 253–81
[3] Forrester P J 2010 *Log-Gases and Random Matrices (LMS-34)* (Princeton, NJ: Princeton University Press)
[4] Serfaty S 2019 Microscopic description of Log and Coulomb gases *Random Matrices* (IAS/Park City Mathematics Series), vol 26 ed A Borodin *et al* (Providence, RI: American Mathmatical Society) pp 34–87
[5] Zabrodin A 2011 Random matrices and Laplacian growth *The Oxford Handbook on Random Matrix Theory* ed G Akemann *et al* (Oxford: Oxford University Press) ch 39
[6] Ameur Y, Kang N-G and Makarov N 2019 Rescaling Ward identities in the random normal matrix model *Constr. Approx.* **50** 63–127
[7] Deelan Cunden F, Facchi P, Ligabò M and Vivo P 2019 Third-order phase transition: random matrices and screened Coulomb gas with hard walls *J. Stat. Phys.* **175** 1262–97
[8] Akemann G and Byun S 2019 The high temperature crossover for general 2D Coulomb gases *J. Stat. Phys.* **175** 1043–65
[9] Fyodorov Y V and Sommers H-J 2003 Random matrices close to Hermitian or unitary: overview of methods and results *J. Phys. A: Math. Gen.* **36** 3303–47
[10] Akemann G 2007 Matrix models and QCD with chemical potential *Int. J. Mod. Phys.* A **22** 1077–122
[11] Fyodorov Y V, Sommers H-J and Khoruzhenko B A 1998 Universality in the random matrix spectra in the regime of weak non-Hermiticity *Ann. Inst. Henri Poincaré* **68** 449–89
[12] van Eijndhoven S J L and Meyers J L H 1990 New orthogonality relation for the Hermite polynomials and related Hilbert spaces *J. Math. Anal. Appl.* **146** 89–98
[13] Di Francesco P, Gaudin M, Itzykson C and Lesage F 1994 Laughlin's wave functions, Coulomb gases and expansions of the discriminant *Int. J. Mod. Phys.* A **9** 4257–351
[14] Tao T and Vu V 2015 Random matrices: universality of local spectral statistics of non-Hermitian matrices *Ann. Probab.* **43** 782–874
[15] Fyodorov Y V, Khoruzhenko B A and Sommers H-J 1997 Almost-Hermitian random matrices: eigenvalue density in the complex plane *Phys. Lett.* A **226** 46–52
Fyodorov Y V, Khoruzhenko B A and Sommers H-J 1997 Almost-Hermitian random matrices: crossover from Wigner–Dyson to Ginibre eigenvalue statistics *Phys. Rev. Lett.* **79** 557–60
[16] Kuijlaars A 2011 Universality *The Oxford Handbook on Random Matrix Theory* ed G Akemann *et al* (Oxford: Oxford University Press) ch 6
[17] Akemann G, Cikovic M and Venker M 2018 Universality at weak and strong non-Hermiticity beyond the elliptic Ginibre ensemble *Commun. Math. Phys.* **362** 1111–41
[18] Życzkowski K and Sommers H-J 2000 Truncations of random unitary matrices *J. Phys. A: Math. Gen.* **33** 2045–57
[19] Osborn J C 2004 Universal results from an alternate random matrix model for QCD with a baryon chemical potential *Phys. Rev. Lett.* **93** 222001

[20] Bender M 2010 Edge scaling limits for a family of non-Hermitian random matrix ensembles *Probab. Theory Relat. Fields* **147** 241–71
[21] Akemann G and Phillips M J 2014 Universality conjecture for all Airy, sine and Bessel kernels in the complex plane *Random Matrix Theory, Interacting Particle Systems, and Integrable Systems* vol 65, ed P Deift and P Forrester (Cambridge: Cambridge University Press) pp 1–24
[22] Ameur Y, Kang N-G, Makarov N and Wennman A 2020 Scaling limits of random normal matrix processes at singular boundary points *J. Funct. Anal.* **278** 108340
[23] Akemann G, Nagao T, Parra I and Vernizzi G 2019 Gegenbauer and other planar orthogonal polynomials on an ellipse in the complex plane (arXiv:1905.02397 [math-ph])
[24] Fox D and Kahn P B 1964 Higher order spacing distributions for a class of unitary ensembles *Phys. Rev.* **134** B1151–5
[25] Nagao T and Wadati M 1993 Eigenvalue distribution of random matrices at the spectrum edge *J. Phys. Soc. Japan* **62** 3845–56
[26] Sommers H-J, Crisanti A, Sompolinsky H and Stein Y 1988 Spectrum of large random asymmetric matrices *Phys. Rev. Lett.* **60** 1895–8
[27] Khoruzhenko B A and Sommers H-J 2011 Non-Hermitian random matrix ensembles *The Oxford Handbook of Random Matrix Theory* ed G Akemann *et al* (Oxford: Oxford University Press) ch 18
[28] Szegö G 1975 *Orthogonal Polynomials* 4th edn (Providence, RI: American Mathematical Society)
[29] Henrici P 1993 *Applied and Computational Complex Analysis* (*Pure and Applied Mathematics* vol 3) (New York: Wiley)
[30] Mason J C and Handscomb D C 2002 *Chebyshev Polynomials* (London: Chapman and Hall)
[31] Olver F W J, Lozier D W, Boisvert R F and Clark C W (ed) 2010 *NIST Handbook of Mathematical Functions* (Cambridge: Cambridge University Press)
[32] Gradshteyn I S and Ryzhik I M 2007 *Table of Integrals, Series, and Products* 7th edn (New York: Academic)
[33] Karp D 2005 Square summability with geometric weight for classical orthogonal expansions *Advances in Analysis, Proc. 4th Int. ISAAC Conf.* ed H G W Begehr *et al* (Singapore: World Scientific) pp 407–21
[34] Forrester P J and Honner G 1999 Exact statistical properties of the zeros of complex random polynomials *J. Phys. A: Math. Gen.* **32** 2961–81
[35] Gaier D 1987 *Lectures on Complex Approximation* (Boston, MA: Birkhäuser) (Translated from German by Renate McLaughlin)
[36] Nehari Z 1952 *Conformal Mapping* (New York: McGraw-Hill)